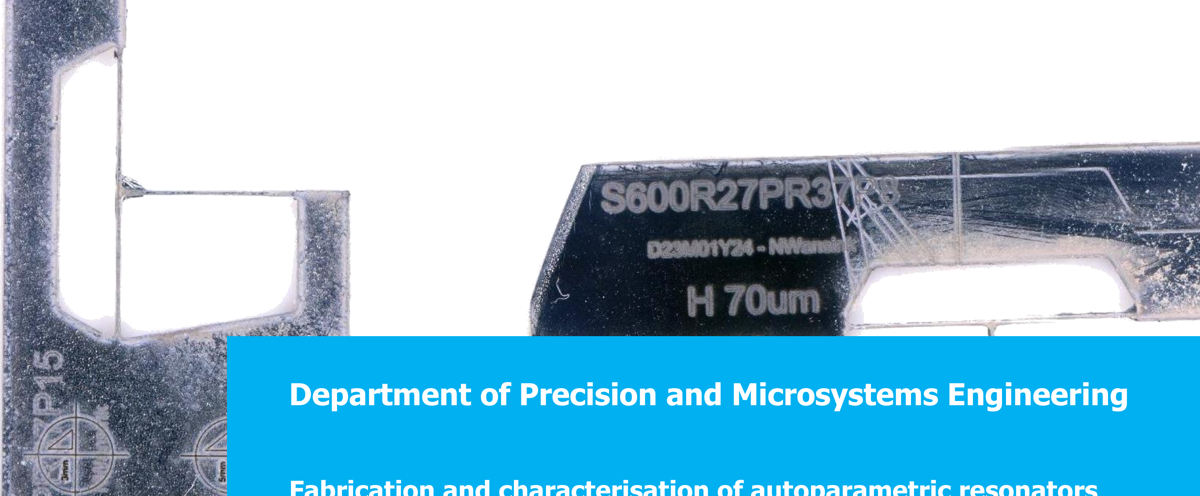

Department of Precision and Microsystems Engineering

Fabrication and characterisation of autoparametric resonators

N. Wansink

Report no	:	2024.014
Coach	:	Zichao Li MSc
Professor	:	Dr. F. Alijani, Dr. D. Farhadi Machekposhti
Specialisation	:	Dynamics of Micro and Nanosystems
Type of report	:	Master thesis
Date	:	22 February 2024

Challenge the future

Fabrication and Characterisation of Autoparametric Resonators

Master's Thesis

Master thesis submitted to Delft University of Technology in partial fulfilment of the requirements for the degree of Master of Science in Mechanical Engineering
Faculty of Mechanical Engineering Technical University of Delft
The Netherlands

By

Nick Wansink

Student High-Tech Engineering,
University of Technology, Delft, The Netherlands,

Student number:	4561805
Project Duration:	14 Februari, 2023 - 29 Februari, 2024
Thesis committee:	Dr. F. Alijani, TU Delft, DMN, supervisor
	Dr. D. Farhadi Machekposhti, TU Delft, DMN, supervisor
	Dr. A. Hunt, MNE, external examiner

An electronic version of this thesis is available at http://repository.tudelft.nl/.

Life can only be understood backwards; but it must be lived forwards.

Søren Kierkegaard

There's plenty of room at the bottom.

Richard Phillips Feynman

Contents

Preface vii

Acknowledgements ix

1 Introduction 1

2 Literature Review 3
2.1 Mode Coupling in micromechanical resonators. 3
2.1.1 Cascade Resonator. 3
2.1.2 T-structure Resonator 4
2.1.3 Coupled Large Mass Resonator 4
2.1.4 Plate Resonator 5
2.2 Femtosecond laser vaporization 7
2.2.1 Material Selection 9
2.3 Conclusion 10

3 Research Methodology 11

4 Paper 15

5 Outlook 25
5.1 Conclusion 25
5.2 Recommendations 26

6 Self reflection 29

Appendix A: Additional reduced order modelling results 37

Appendix B: Additional fabrication results 41

Appendix C: Additional measurements results 45
C.1 Doubly Clamped Beam Resonators 45

Preface

In this thesis, the dynamics and fabrication of microsystems are studied. Microsystems play a vital role in our lives. On the one hand, microsystems such as accelerometers are used daily, in our cellphones to count steps or change the orientation of the viewing screen. On the other hand, the development of smaller and integrated microsystems is still ongoing, reaching quantum levels. This thesis aims to cover a small portion of the ongoing research. I hope that during reading, you will be as fascinated by the dynamics of microsystems as I have been.

ACKNOWLEDGEMENTS

The past seven and a half year, I have had the great opportunity to study and work at one of the best (technical) universities in the world. This experience has led me to write this thesis in a fantastic environment.

Firstly, I am very grateful to dr. Farbod Alijani as he has been my supervisor during my master and bachelor thesis. His incredible guidance could not be understated. I hope our future collaboration will be as successful and pleasant.

Secondly, I would like to thank dr. Davood Farhadi Machekposhti for our fruitful discussions, even when he is currently very busy in the United States.

Thirdly, I would like Zichao MSc for the supervision during this project. We had many fantastic and fruitful discussion about this project and many unrelated topics.

Furthermore, I would like to thank dr. Ata Keşkekler and Ruben Guis MSc for their help with the Laser Doppler Vibrometer, and all technical and support staff, especially Gideon Emmaneel who has often been available for discussions concerning the Lasea.

Lastly, I would like to thank my friends and family for their support. Especially, my girlfriend Susan van den Dool has been supporting me throughout my whole study career. I am grateful to have so many incredible people around me.

Nick Wansink
Delft, February 2024

1

INTRODUCTION

In 1959, R.P. Feynman presented a lecture titled "*There's plenty of room at the bottom*", referring to the miniaturisation of technology [1]. The miniaturisation of technical devices has certainly received widespread attention for several decades, especially mechanical resonators due to the sensitivity and low energy dissipation [2]. These devices, which are nowadays broadly classed as microsystems or MEMS and NEMS, have become feasible on micro and nanoscale due to the availability of several techniques, e.g. additive manufacturing and lithography [3–6]. Applications of micro- and nanomechanical resonators are commonly used for ultrasensitive force and mass sensing, narrow band filtering and time keeping [7, 8]. Furthermore, microsystems are generally monolithic, since assembly on submilimeter scale by human hand is difficult - if not impossible - to perform [9]. The compliance of the material is therefore exploited to enable fabrication and form complaint mechanisms. Compliant mechanisms provide a monolithic, high precision and frictionless solution [10] and often exhibit geometrical nonlinearities due to the large deflections [11].

An interesting phenomenon occurring in highly nonlinear micromechanical resonators is mode coupling due to autoparametric resonance, which cannot be observed in linear dynamics. Autoparametric resonance refers to the exchange of energy between (fundamental) modes due to the presence of nonlinearity, while the ratio of the eigenfrequencies of these modes is rational [4]. The nonlinearities and driving force of a resonator have to be sufficiently strong to allow for appreciable coupling between modes already at low energies. In contrast to internal resonance which is a general form of mode coupling, autoparametric resonance is caused by a force that has the same form as the stiffness modulated at twice the frequency. While parametric excitation is due to an external force, autoparametric is caused by the resonator itself [12].

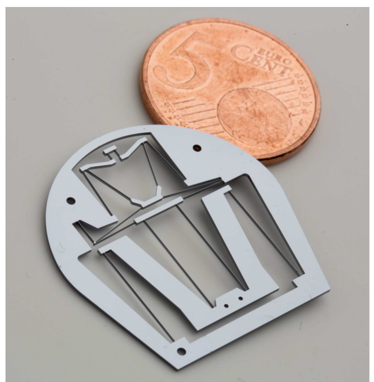

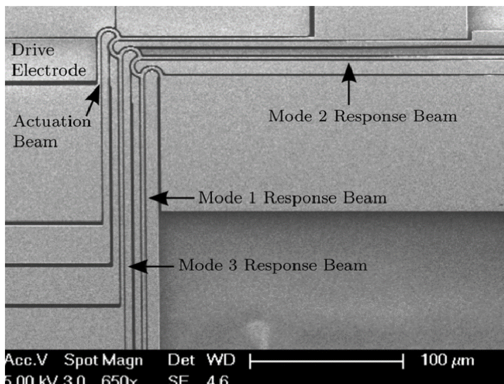

Figure 1.1: Several monocrystalline silicon micromechanical resonators. (a) A compliant Frequency-Quadrupler transmission used for frequency multiplication [10]. (b) A compliant micromechanical resonance cascade used for multi-stage frequency division. [13]

Mode coupling has already been studied in micromechanical systems [14–16] for many application, such as mass sensing, sensing of angular rate signals [17], inertial sensing [18], energy harvesting [19], noise suppression [20], frequency stabilisation [21], generate frequency combs [22] in addition to filtering [13, 23, 24]. However, many of these resonators are fabricated using dry reactive ion etching [25], while alternative fabrication techniques offer advantages such as faster prototyping without the need for a clean room and the ability to fabricate complex three dimensional structures. A suitable fabrication technique that harnesses these attributes is femtosecond laser vaporization. Furthermore, mode coupling is often achieved by applying optothermal forces [22] or by manipulating the geometry. While the former is very susceptible to changes in tension and upon heating by external forces may become absent, the latter is tedious to achieve [13, 15, 26]. Therefore, laser Doppler vibrometry is used as a viable alternative to these measurement techniques [27] [28].

This paper therefore formulates and evaluates a method to fabricate micromechanical resonators by femtosecond laser vaporization and characterise them by laser Doppler vibrometry. Specifically, autoparametric resonance in a micromechanical resonator is studied.

This thesis has the following structure. In chapter 1, a brief introduction to the subject of this thesis is provided. Subsequently, a literature review on the current state of mode coupling is presented in chapter 2. In chapter 3, the research question, research objectives and research methodology are shown. Chapter 4 is used to present and discuss the findings of this study. In chapter 5, conclusions and recommendations are drawn based on the obtained research. The last chapter, chapter 6, finalises with a brief self reflection on this thesis process.

2

Literature Review

In this chapter, we introduce the research topic, present the current state of research, and highlight identified research gaps. The first section provides a short overview of mode coupling in micromechanical resonators. Subsequently, we discuss femtosecond laser vaporization and relevant studies. To conclude this section, we summarise the findings and insights in the following conclusion.

2.1. Mode Coupling in micromechanical resonators

The past decade, a diverse range of micro mechanical structures have been designed to achieve mode coupling [13–24]. In this section, several of these structures and their applications are shown. In Table 2.1 is included - if possible - the fundamental frequency f_0, the ratio between frequencies, the Q-factor Q_0, the span and depth of the whole resonator (excluding the supporting material), the smallest feature size (SFS), material (Mat) and fabrication (Fab) and measuring (Meas) techniques.

Resonator Type	f_0 (kHz)	Ratio	Q_0 (µm^2)	Span size (m)	Depth (µm)	SFS	Mat	Fab	Meas
Cascade [13]	105	$1:2^N$	858	400×400	10	1.85	Si	DRIE	LDV
T-structure [24]	-	$1:2^N$	-	300×196	20	2	Si	-	-
Coupled Large Mass [16]	11.7	$1:3$	2.92	354×160	3.5	2	-	-	CC
Disk [15]	251	$1:2$	$8\cdot10^4$	600	40	1.5	Si	-	CC
Plate[1] [14]	3.42	$1:1$	10	$1.633a^2$		-	-	-	-

Table 2.1: CC: Capacitance change

2.1.1. Cascade Resonator

Frequency division can be achieved by a micromechanical resonance cascade which is shown in Figure 2.1. Finite deformations of the beam ends provide the necessary non-

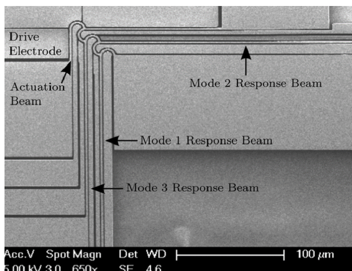

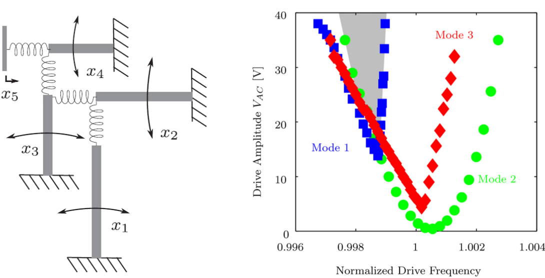

Figure 2.1: The Cascade Resonator. Driving element x_5 parametrically excites element $x4$, which parametrically excites element x_3, and so on down to element x_1, with frequency division by 2 at each stage. Resonant response amplitudes are dictated by system nonlinearities. [13] (a) SEM micrograph of the Cascade Resonator, with $400\mu m \times 400\mu \times 10\mu m$ and a feature size of $1.85\mu m$. (b) Schematic model of a multi-stage frequency divider with four localised modes and coupling spring elements. (c) Normalised modal parametric instability boundaries for modes 1, 2 and 3 with frequencies normalised by modal number n. Divide-by-eight operation is achieved in the shaded overlap region.

linear modal coupling. A harmonic signal is applied to the actuation beam (x_5) which produces a parametric response in the next beam (x_4) at half the input frequency. This beam also produces a parametric response down to element x_1. [13][26]

Interestingly, the instability regions in Figure 2.1c do not represent single mode parametric resonance regions due to the fact that the modal responses include the dynamics of other modes. The element x_4 will predominantly be driven by parametric excitation, while element x_3 will be largely driven by the driving force due to their alignment with respect to the actuation element x_5, causing the instability regions as shown.

2.1.2. T-STRUCTURE RESONATOR

Frequency division can also be achieved by a similar structure such as the T-shaped structure in Figure 2.2. This structure is based on the previous cascade and other papers. However Dou et al. [24] used a structural optimisation algorithm to enhance the mode coupling in this structure resulting in the figures shown. In this structure, the geometric nonlinearity increases, since the axial deformation along the vertical beam increases due to a larger end mass and a thinner cross section relative to the initial design.

2.1.3. COUPLED LARGE MASS RESONATOR

Yan et al. explore the regime in which energy is supplied to the upper mode for systems at internal resonance. When the nonlinear coupling transfers energy from the higher mode to the lower mode, stable vibrations are induced in the latter with a period that is an integer multiple of the period of the drive.

Using an electromechanical resonator with two modes at internal resonance, the nonlinear coupling leads to an effective parametric modulation on the lower mode, which is resonantly enhanced by the higher mode. Upon activation, energy can be transferred from the higher mode to the lower mode to excite oscillations in the latter with a resonance ratio of 1 : 3. [16]

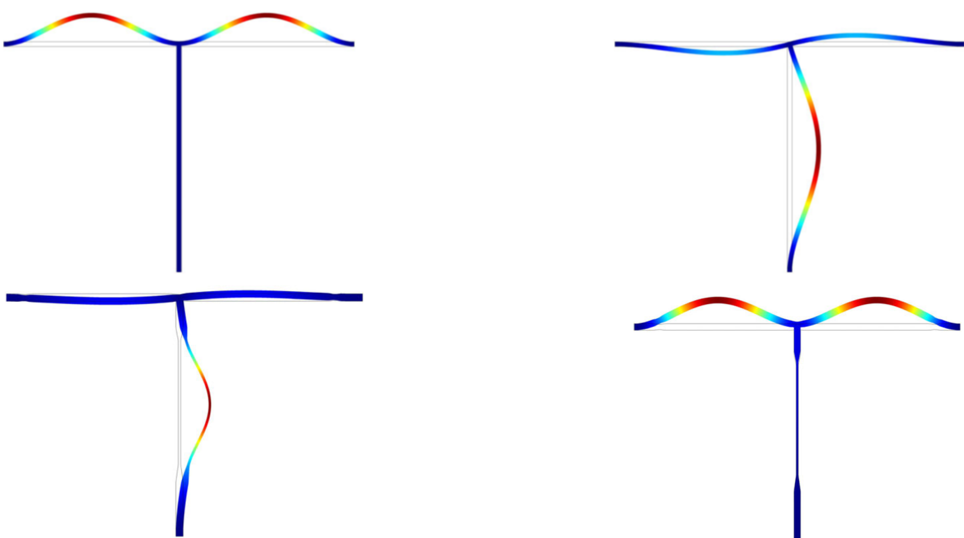

Figure 2.2: A mode coupled T-structure: an initial and optimised design to maximise the absolute value of the essential modal coupling coefficient and the two coupled linear vibration modes, where $\omega_2 = 2\omega_1$. (a) Initial design: Linear vibration mode 1 (ω_1). (b) Initial design: Linear vibration mode 2 (ω_2). (c) Optimised design: Linear vibration mode 1 (ω_1). (d) Optimised design: Linear vibration mode 2 (ω_2).

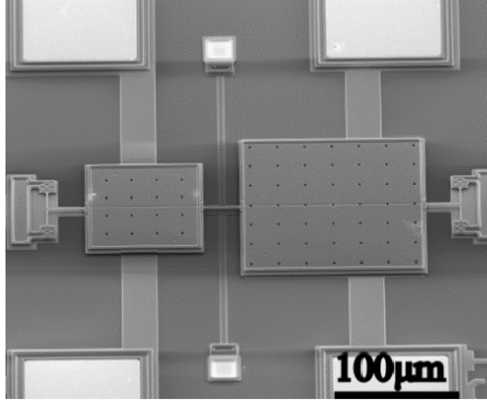

Figure 2.3: A Two-Rectangle Resonator

2.1.4. PLATE RESONATOR

In the work of Chang et al., the dynamic response of a rectangular plate to harmonic excitations is investigated [14]. Since certain aspect ratios between side lengths of a plate will create two or more modes with identical frequencies, mode coupling could be achieved in a plate as well. The relative simple geometry is an interesting shape for this application. As shown in Figure 2.4, for an aspect ratio of $\kappa = 1.633$, both eigenfrequencies are $p_1 = p_2 = 3.42$, thus achieving a ratio of $1:1$.

Steady-state solutions of the averaged equations are studied in considerable detail. Emphasis in their work is on determining the conditions which lead to mode coupling. It is shown that, depending on the mode combinations in response, as well as the mode that is excited, qualitatively distinct response diagrams can be obtained. Stable single-mode and coupled-mode responses are found to coexist over a wide frequency interval.

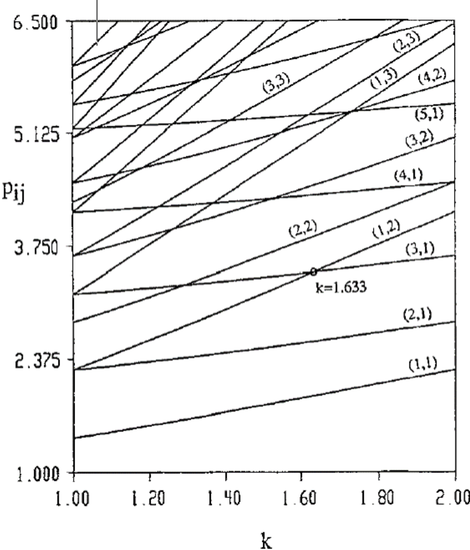

Figure 2.4: Dependence of linear natural frequencies for the various plate modes on the aspect ratio κ

2.2. FEMTOSECOND LASER VAPORIZATION

Fabrication of MEMS is often done by DRIE (Deep Reactive-Ion Etching) [25] [29]. DRIE is a high precision fabrication method at micro- and nanoscale (0.1 µm - 100 µm) with an etch rate for silicon of 50 µm/min [30]. For nanomechanical structures, this rate is sufficient. For micromechanical structures in the range of more than 10 µm however, this process can take several hours.

Another fabrication method that can be used is femtosecond laser vaporization, especially for structures at microscale (10 µm - 1000 µm). The fabrication time can be decreased by 100 with respect to fabrication by DRIE, as has been experienced during early prototyping. Advantages of the DRIE such as a high aspect ratio (the slope of the vertical edge) can be recreated by precession of the laser.

Femtosecond laser vaporization is a fabrication method in which the material is directly vaporised due to the very short times scales involved in the vaporization. It has been shown that the time scale for the fast electron cooling and a considerable energy transfer to the lattice is of the order of 1 ps. During the vaporization, thermal conduction into the bulk material can be neglected in a first approximation [31]. In Figure 2.5, vaporization of a 0.3 mm thick silicon target is shown with a different set of pulses.

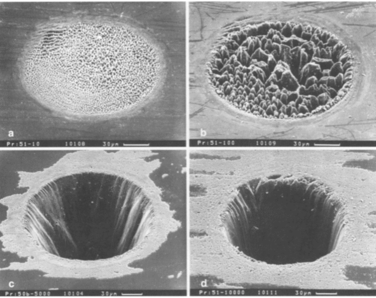

Figure 2.5: Vaporization of a 0.3 mm thick silicon target with: (a) 10, (b) 100, (c) 5×10^3 and (d) 10^4 pulses [31]

Several parameters have been found to be significant. Parameters considered here are the fluence, repetition rate, pulse duration, energy dose per millimetre and scanning velocity [32]. These parameters influence the etch rate (in µm^3 per pulse), the vaporization efficiency and the processing quality.

FLUENCE

Fluence is the pulse energy per spot area in J/cm^2 and influences both the kinetic and quality of vaporization. The etch rate increases with the fluence as is also shown in 2.6a for stainless steel. For this particular material, a slope change occurs at 1 J/cm^2 due to a transition between the optical and the thermal regime [31]. Furthermore, the width of the groove increases with fluence due to the Gaussian spatial profile of the laser beam.

The efficiency of vaporization decreases with an increasing fluence or an increasing pulse duration. Moreover, the processing quality is significantly decreased at high fluence. Two causes are heat accumulation, which improves the etch rate while damaging the surrounding material, and particles shielding, which reduces the pulse energy available to produce vaporization. Therefore, a fluence lower than the transition between the optical and thermal regime should be used.

SCANNING VELOCITY

Lopez et al. [32] qualitatively analysed SEM pictures of a stainless steel foil in which several groves were engraved with different scanning velocities. It was showed that the

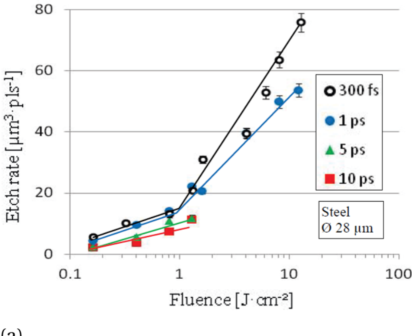

(a)

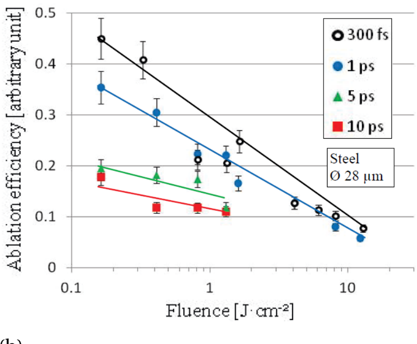

(b)

Figure 2.6: The effect of fluence on vaporization for a pulse duration ranging from 300 fs to 10 ps on a stainless steel target. Repetition rate used is 2 MHz up to 1.3 J/cm^2 then 200 kHz for higher fluencies [32]. (a) Maximum etch rate versus fluence (b) Maximum vaporization efficiency versus fluence

thermal load deposited into the material increases with decreasing scanning velocity. As soon as the actual velocity becomes smaller than a certain velocity, melting will occur inside and in the vicinity of the groove. Then extensive burrs, droplets and roughness will appear. At very low velocities, the groove will ultimately collapse and the laser is not engraving anymore.

ENERGY DOSE PER MILLIMETRE

For a certain repetition rate, energy and scanning velocity, a value that Lopez et al. called *dose* can be calculated by Equation 2.1 with units J/mm. For a material, a critical dose exists beyond which there is a drastic drop in etch rate per fluence, and a maximum dose beyond which the groove collapses due to melting and there is no engraving anymore. Thus, high velocity and low energy (which is tied to the fluence) reduce the dose and increase the process quality.

$$Dose = \frac{Repetition\ Rate \times Energy}{Scanning\ Velocity} \tag{2.1}$$

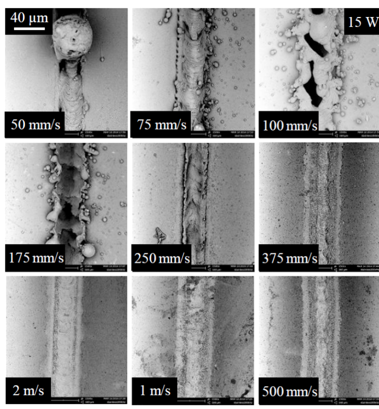

Figure 2.7: SEM pictures of a stainless steel foil engraved with scanning velocities ranging from 50 mm/s to 2 m/s. Average power is 15 W, repetition rate is 200 kHz and pulse duration is 300 fs [32].

THERMAL DAMAGE CRITERION

Another study to the femtosecond laser vaporization showed a criterion which predicts the thermal damage. The criterion is determined by the total thermal energy absorbed per surface point upon irradiation Q, the scanning velocity v and the pulse-to-pulse distance Δx as shown in Equation 2.2. This approach assesses both the energy absorbed by the surface as well as the duration of irradiation [33].

$$C_{td} = \frac{Q}{v\Delta x} \tag{2.2}$$

This approach is used in Figure 2.8, in which the temperature gradient is represented by the middle figure and the thermal damage criterion by the right figure. The left figure clearly corresponds with the right figure.

Furthermore, a high thermal damage criterion seems to relate to a combination of a high melting point, a low heat capacity and a low thermal diffusivity [33]. For the stainless steel 316L shown in Figure 2.8, these are respectively 1400 °C, 472 J/(kgK) and 3.9×10^{-6} m^2/s.

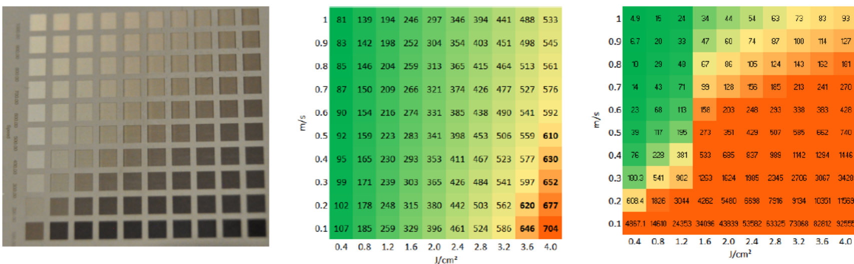

Figure 2.8: (Left) Matrix of ablated areas (stainless steel 316L) using peak fluences in the range of 0.4 J/cm^2 to 4 J/cm^2 (left to right) and scanning speeds varying from 0.1 m/s to 1 m/s (bottom to top) at 500 kHz pulse repetition rate, 14 µm spot diameter at focus, 5 µm pitch and 5 layers. The area of each square is 1.5 mm ×1.5 mm. (Middle) The simulated temperatures' colours were chosen so that areas at which the temperature exceeds 600 °C are orange. (Right) The simulated absorbed heat colours chosen are yellow if $Ctd > 70\ MJs$ and orange if $Ctd > 200$ MJs (and green otherwise) for fluences above 1.6 J/cm^2 (high fluence range), and yellow if $Ctd > 400$ J/cm^2 and orange if $Ctd > 2000$ J/cm^2 for the lower fluence range.

2.2.1. MATERIAL SELECTION

Monocrystalline silicon (Si) is the single material most widely used in MEMS fabrication [34]. Si has excellent mechanical properties, low intrinsic damping due to its purity and can be process in batches at low costs. Furthermore, the material is compatible with electric components such as semiconductors [4].

The properties of monocrystalline silicon are E = 165.6 GPa and ρ = 2330 kg/m^3, with the Young's modulus in the direction of the principal axis. We assume a linear stress-strain law and uniform material properties. However, due to the fabrication of monocrystalline silicon wafers, the Young's modulus is directional and should be taken into account [34].

The melting point, heat capacity, thermal diffusivity and thermal conductivity are respectively 1685 °C, 712 J/(kgK) [35], 89×10^{-6} m^2/s and 148 W/(m·K) [36].

2

2.3. CONCLUSION

Micromechanical resonators have shown to exhibit interesting phenomena at high nonlinearity. Particularly, autoparametric resonance can be seen in several devices for numerous applications. However, many of these devices are fabricated using DRIE, deep reactive ion etching. This fabrication process is tedious, relatively inaccessible and slows prototyping due to long fabrication duration.

In contrast, femtosecond laser vaporization has shown to be a promising fabrication alternative due to its accessibility and fast fabrication. However, this fabrication technique isn't generally utilised in the fabrication of MEMS, especially not to achieve highly nonlinear resonators. Therefore, this literature review concludes that a research gap exists in the fabrication of highly nonlinear MEMS by femtosecond laser vaporization. This research gap can be subdivided in the following relevant research gaps that have been identified:

- To study femtosecond laser vaporization of monocrystalline silicon wafers
- To determine three fabrication parameters to cut monocrystalline silicon [2], which are:
  - Fluence (or power)
  - Scanning velocity
  - Repetition rate
- To investigate the effect of femtosecond laser vaporization on:
  - Geometry
  - Material
- To study the frequency response of micromechanical resonators fabricated by femtosecond laser vaporization
- To study nonlinearity in a micromechanical resonator
- To study autoparametric resonance in a micromechanical resonator

Two distinct research question will be investigated in this following paper to address the aforementioned research gap and its subdivisions.

1. **How to fabricate and characterise a micromechanical resonator by femtosecond laser vaporization?**
2. **Is it possible to measure autoparametric resonance in a micromechanical device fabricated by femtosecond laser vaporization?**

[2] The material parameters and methodology are not exclusive to silicon.

3

Research Methodology

As discussed in the literature review in chapter 2, two distinct questions will be investigated:

1. **How to fabricate and characterise a micromechanical resonator by femtosecond laser vaporization?**
2. **Is it possible to measure autoparametric coupling in a micromechanical device fabricated by femtosecond laser vaporization?**

These research questions will be answered with a protocol shown in Figure 3.1. This protocol, similar to Keşkekler *et al.* [22], combines a computational analysis to determine the frequency response of a designed resonator and an experimental study to characterise the fabricated resonator. The subsequent steps are taken to develop, fabricate and characterise these resonators:

1. A Finite Element Model (FEM) of a micromechanical resonator is computed using COMSOL;
2. A sample of the resonator based on the FEM is fabricated by femtosecond laser vaporization;
3. An updated FEM is made, based on the fabrication test. This process is repeated until a recipe is developed to fabricate a micromechanical resonator;
4. A Reduced Order Model (ROM) [37] is calculated from the FEM in MATLAB;
5. A frequency response is determined by Matcont based on the ROM in MATLAB;
6. A measurement is performed on the fabricated resonator wit laser Doppler vibrometry [27];
7. The experimental and computational data are compared and validated;

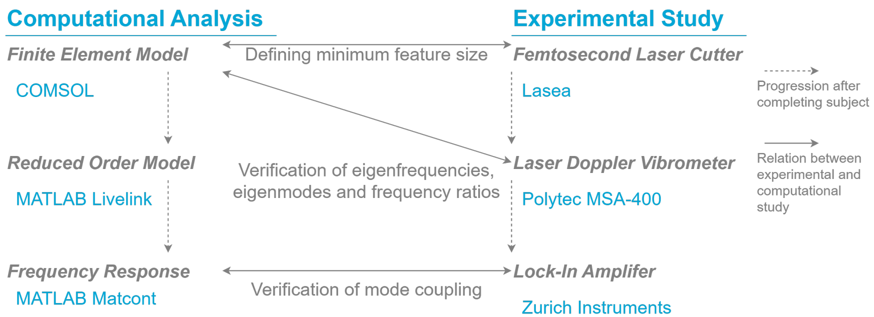

Figure 3.1: Protocol to fabricate and measure micromechanical resonators by using a combination of software and hardware.

COMPUTATIONAL ANALYSIS

The computational analysis is utilised to determine the frequency response and validate the experimental results of a micromechanical resonator. The frequency response is calculated by Matcont based on a Reduced Order Model, which is in turn determined based on a finite element model in COMSOL. The code used to generate the ROM is developed by Bos and Steeneken [37] and based on *STEP* (Stiffness Evaluation Procedure).

Importantly, the requested modes with complementary quality factor and driving frequency should be entered, next to the driving force.

FEMTOSECOND LASER VAPORIZATION

The resonators are fabricated by femtosecond laser vaporization of monocrystalline silicon wafers using precession as shown in Figure 3.2. Precession is used to orient the laser with rotating mirrors (Figures 3.2b and 3.2c) at an angle with respect to the wafer in order to cut vertical edges, which would be impossible with a vertically pointed laser. During the fabrication process, the wafer is oriented so that the positive orientation (flat end) is aligned with the top of the micromechanical resonator since the crystal orientation of the silicon wafer has significant effect on the fabrication properties and subsequent measurement results [34].

The use of precession results in a total line or trench thickness of 75 µm as shown in 3.2c due to the spot diameter of 15 µm and ring shape diameter of 60 µm. Furthermore, by using three outlines with a pitch of 10 µm efficiency is improved and trench depth per repetition increased, while minimising trench thickness. The added thickness to the beam should thus be 95 µm, since the laser assumes this line as its middle point. From empirical research in this study however, an added thickness of 60 µm is advised (Appendix A).

As shown in 3.2d, the micromechanical resonators consist of three parts. Each part is fabricated by a different set of parameters. Firstly, the resonator itself (blue) is cut with a smooth cut. High scanning velocity and low power decrease the local heating, although the duration is increased drastically [32, 33]. This recipe is highly suitable to cut small features. Secondly, the base in green is fabricated with a rough cut to decrease fabrication time. This recipe causes much local material degradation and would therefore not be suitable for small features. Thirdly, text is engraved on the base containing the first

parameters, date and designer. Additionally, design specifications and reference circles can be engraved. To engrave readable text, the precession mode should be shut off.

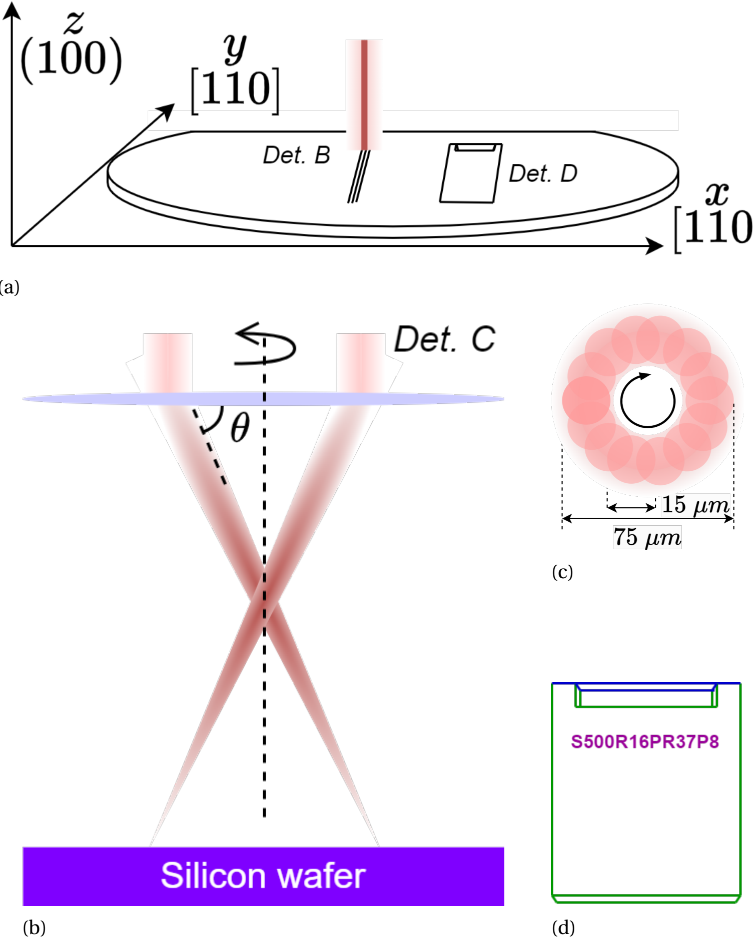

Figure 3.2: Schematics of the operation of the Lasea femtosecond laser cutter. (a) Fabrication set-up with wafer orientation [34] including the femtosecond laser along one of three lines with a pitch of 10 μm between lines. (b) The use of precession with an angle of attack of 65 deg resulting in a ring shape with a diameter of 60 μm and spot diameter of 15 μm. Thus, the total thickness of a line (trench) is 75 μm. (c) Illustration of the ring-shaped laser spot due to precession of the laser. (d) The different line colours of the micromechanical resonator correspond with the parameters presented in Table B.1 with green for a rough cut, blue for a smooth cut and purple for engraving.

Laser Doppler vibrometry

A Polytec MSA-400 Laser Doppler Vibrometer is used to characterise micromechanical resonators [28] as shown in Figure 3.3. The micromechanical structure, presented in Figure 3.4, is placed on a base with a piezo shaker in a vacuum chamber with a Pfeiffer vacuum system which results in a vacuum of 10^{-4} mbar. The LDV senses the frequency

shift of back scattered light from the moving surface, thus providing the frequency response curves. The out-of-plane eigenmodes and their eigenfrequencies modelled in COMSOL are compared and verified to the results from Polytec.

A Lock-in amplifier from Zurich Instruments is used in combination with the LDV to investigate the nonlinearity and mode coupling in the micromechanical resonators. The settling time is $\tau = Q/\omega$, which is approximately 10 ms for resonators with a quality factor of 100 and frequency range of 10 kHz. Furthermore, a band-pass filter of 100 Hz is used (which is actually a low-pass filter due to the mechanics of the Lock-in).

Actuation for both characterisation and operation is done by base excitation and provided by a piezo shaker with a maximum applied voltage of 100 V which is resonating the micromechanical resonator vertically (in-plane) as shown in Figure 3.3. The velocity of one or multiple points on each beam (in-plane) are detected using a Polytec MSA-400 Laser Doppler Vibrometer. Multiple points are used to characterise the frequency spectrum and eigenmodes to verify the FEM simulations. Single point measurements are used to determine modal parameters by sweeping ω_d for different magnitudes of V. Both measurements require different runs for each beam due to the single point laser.

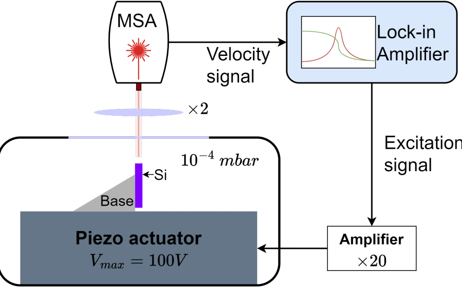

Figure 3.3: Schematic of the measurement set-up comprising of a Polytec MSA-400 LDV and Lock-in Amplifier for reading-out the motion and a piezo actuator in a vacuum chamber for generating the excitation force with a maximum voltage of 100 V [27].

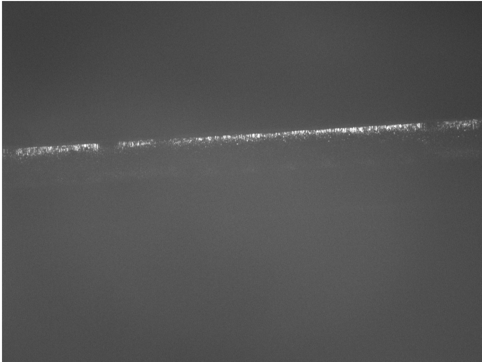

Figure 3.4: Image of a resonator in the LDV set-up of Figure 3.3. The part of the beam that shows reflection, generally produces the best signal, resulting in sufficient back scattered light to detect a frequency shift.

4

Paper

Fabrication and characterisation of autoparametric resonators

Nick Wansink[1], Farbod Alijani[1], Davood Farhadi Machekposhti[1], Zichao Li[1]

[1] *Department of Precision and Microsystem Engineering, Delft University of Technology, 2628 CD Delft, The Netherlands*

23rd February 2024

ABSTRACT

Micromechanical resonators, which have become feasible due to advanced manufacturing techniques, have shown several interesting phenomena including mode coupling in a range of applications that span metrology and sensing. Conventional fabrication methods of these resonators have been used throughout the field. However, fabrication of micromechanical resonators by femtosecond laser ablation which could accelerate prototyping, access to three dimensional resonators and reduce clean room use, has received little attention.

In this study, a protocol for fabricating and measuring laser cut micromechanical resonators using computational analysis and experimental techniques has been developed and validated through comparison with previous works by characterising doubly clamped beam resonators. The fabricated prototype is demonstrated to exhibit autoparametric resonance and coupling showcasing the potential of the new approach in engineering and fast prototyping of coupled micromechanical resonators.

I. INTRODUCTION

In 1959, R.P. Feynman presented a lecture titled "*There's plenty of room at the bottom*", referring to the miniaturisation of technology [1]. The miniaturisation of technical devices has certainly received widespread attention for several decades, especially mechanical resonators due to the sensitivity and low energy dissipation [2]. These devices, which are nowadays broadly classified as microsystems or MEMS and NEMS, have become feasible on micro and nanoscale due to the availability of several techniques, e.g. additive manufacturing and lithography [3–6]. Applications of micro- and nanomechanical resonators are commonly used for ultrasensitive force and mass sensing, narrow band filtering and time keeping [7,8]. Furthermore, microsystems are generally monolithic, since assembly on submilimeter scale by human hand is difficult - if not impossible - to perform [9]. The compliance of the material is therefore exploited to enable fabrication and form complaint mechanisms. Compliant mechanisms provide a monolithic, high precision and frictionless solution [10] and often exhibit geometrical nonlinearities due to the large deflections [11].

An interesting phenomenon occurring in highly nonlinear micromechanical resonators is mode coupling due to autoparametric resonance, which cannot be observed in linear dynamics. Autoparametric resonance refers to the exchange of energy between (fundamental) modes due to the presence of nonlinearity, while the ratio of the eigenfrequencies of these modes is rational [4]. The nonlinearities and driving force of a resonator have to be sufficiently strong to allow for appreciable coupling between modes already at low energies. In contrast to internal resonance which is a general form of mode coupling, autoparametric resonance is caused by a force that has the same form as the stiffness modulated at twice the frequency, similar to parametric resonance. While parametric resonance is due to an external force, autoparametric resonance is caused by the resonator itself [12].

Mode coupling has already been studied in micromechanical systems [13–15] for many application, such as mass sensing, sensing of angular rate signals [16], inertial sensing [17], energy harvesting [18], noise suppression [19], frequency stabilisation [20], generate frequency combs [21] in addition to filtering [22–24]. However, many of these resonators are fabricated using dry reactive ion etching [25], while alternative fabrication techniques offer advantages such as faster prototyping without the need for a clean room and the ability to fabricate complex three dimensional structures. A suitable fabrication technique that harnesses these attributes is femtosecond laser vaporization [26]. Furthermore, mode coupling is often achieved by applying optothermal forces [21] or by manipulating the geometry. While the former is very susceptible to changes in tension and upon heating by external forces may become absent, the latter is tedious to achieve [14,23,27]. Therefore, laser Doppler vibrometry is used as a viable alternative to these measurement techniques [28] [29].

This paper therefore formulates and evaluates a method to fabricate micromechanical resonators by femtosecond laser vaporization and characterise these by laser Doppler vibrometry. Specifically, autoparametric resonance in a micromechanical resonator is studied. In section II, the research method is discussed. Subsequently, fabrication results are shown in section III. The measurement results are examined in section IV. Concluding with section V, a brief conclusion is presented.

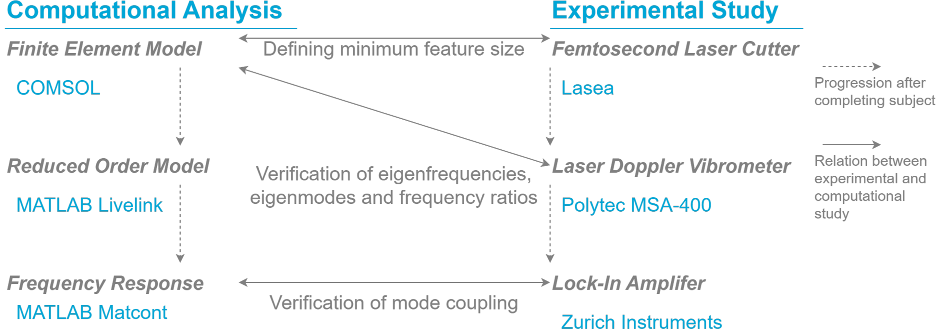

Fig. 1: Protocol to fabricate and characterise micromechanical resonators by using a combination of software and hardware.

II. METHOD

In this study, a model of a micromechanical resonator is developed and fabricated to examine mode coupling through its geometric nonlinearity achieving autoparametric coupling, as shown in Figure 1. To achieve these objectives, a continuum model in the FEM software COMSOL is designed. Thereafter, a Reduced Order Model of the continuum model is created by MATLAB package via Livelink, which is a Stiffness Evaluation Procedure [30]. To obtain the frequency response curves and determine mode coupling, the Matcont package in MATLAB is used. For more information regarding these ROM simulations, the reader can review the following articles [21] [29].

Secondly, the model is fabricated out of monocrystalline silicon wafers using femtosecond laser vaporization from Lasea. The wafer thickness varies between 380 µm and 500 µm. The resulting structure is examined under a Keyence Digital Microscope VHX-6000.

To verify mode coupling in the micromechanical resonators, a Polytec MSA-400 Laser Doppler Vibrometer is operated. The micromechanical structure is placed on a base with a piezo shaker in a vacuum chamber with a Pfeiffer vacuum system. The LDV senses the frequency shift of back scattered light from the moving surface, thus providing the frequency response curves. The out-of-plane eigenmodes and their resonance frequencies modelled in COMSOL are compared and verified to the results from Polytec.

A Lock-in amplifier from Zurich Instruments is used in combination with the LDV to investigate the nonlinearity and mode coupling in the micromechanical resonators.

The micromechanical resonators that will be studied are a doubly clamped beam resonator [24,31] and an optimised frequency divider proposed by Dou *et al.* [24], which resembles a T-shape as shown in Figure 2. The former resonator is used to validate the fabrication and measurement method. The frequency divider will be studied since it has been numerically proven to show mode coupling, yet experiments still have to verify the presence of mode coupling in this resonator. Furthermore, the T-shaped resonator benefits from a combination of internal resonance and geometrical coupling in a single micromechanical resonator, and could thus present autoparametric resonance. Finally, such a resonator could be linked by n elements in order to achieve division by 2^n [23].

The dynamics are realised by two microbeam elements that are perpendicular in order to resemble a T-shape as shown in the finite element model in Figure 2. The ends of the beams are all clamped. The horizontal and vertical beam are geometrically coupled at its centre and end, respectively. = Small semi-circular notches are cut out at the ends of the horizontal beam as well as a wide recessed beam along the centre of the vertical beam.

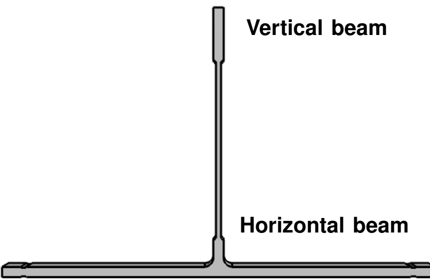

Fig. 2: Schematic of a T-shaped resonator [24], which spans $5\ mm \times 3\ mm$ with a uniform depth of 380 µm.

Due to the T-shaped design, two localised vibrational modes can exchange energy when their resonance frequencies are (approximately) commensurable. One localised mode is located in the vertical beam (Figure 3a), the other in the horizontal beam (Figure 3b). In this case, the first mode is located in the vertical beam. The most efficient energy transfer occurs when the ratio of the frequencies of the horizontal and vertical beam is $f_1 = 2f_2$ or vice versa [12]. By driving the resonator with a harmonic load at a frequency close to f_2, the first mode will

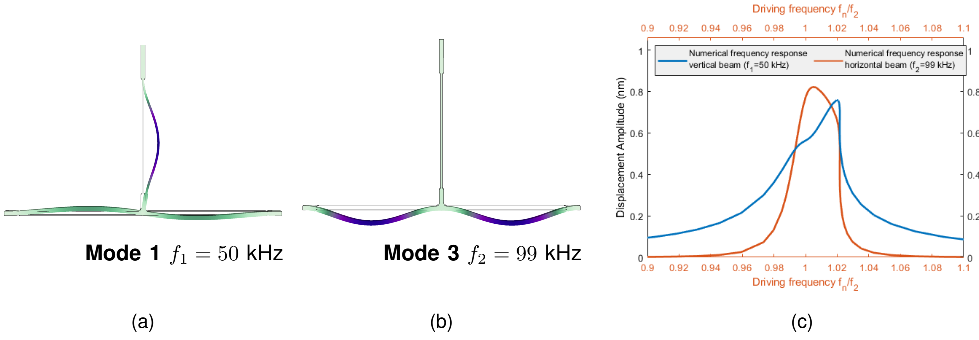

Fig. 3: (a) First vibrational mode in the vertical beam by FEM (b) Third vibrational mode in the horizontal beam by FEM. (c) Frequency response by using a reduced order model of a finite element model in COMSOL of a T-shaped resonator. The first mode at 50 kHz (blue) is induced by the third mode at 99 kHz (red), while driven at the resonance frequency of the third mode.

be actuated leading to autoparametric coupling as shown in the frequency response of a reduced order model of the T-shaped resonator in Figure 3c. When the amplitude of the third mode - the horizontal beam - is sufficiently large, vibration of the first mode - the vertical beam - will be induced due to parametric pumping. The transverse vibration of the horizontal beam provides an axial force in the vertical beam, which in turn induces transverse motion of the vertical beam when the frequency of the horizontal beam is approximately twice that of the vertical beam. Importantly, the frequency response of both modes is shown at the driving frequency in Figure 3c. When shown at the analysing frequency - the frequency at which a measurement will take place - the modes are detected at their respective resonance frequency.

III. FABRICATION BY FEMTOSECOND LASER VAPORIZATION

The resonators are fabricated by femtosecond laser vaporization of monocrystalline silicon wafers using precession as shown in Figure 4. Precession is used to orient the laser with rotating mirrors (Figures 4b and 4c) at an angle with respect to the wafer in order to cut vertical edges, which would be impossible with a vertically pointed laser. During the fabrication process, the wafer is oriented so that the positive orientation (flat end) is aligned with the top of the micromechanical resonator since the crystal orientation of the silicon wafer has significant effect on the fabrication properties and subsequent measurement results [32].

The use of precession results in a total line or trench thickness of 80 µm as shown in Figure 4c due to the spot diameter of 15 µm and ring shape diameter of 60 µm. Furthermore, by using three outlines with a pitch of 10 µm efficiency is improved and trench depth per repetition increased, while minimising trench thickness. The added thickness to the beam should thus be 95 µm, since the laser assumes this line as its middle point. From empirical research in this study however, an added thickness of 60 µm is advised.

As shown in Figure 4d, the micromechanical resonators consist of three parts. Each part is fabricated by a different set of parameters shown in Table I. Firstly, the resonator itself (blue) is cut with a smooth cut. High scanning velocity and low power decrease the resulting residual stress in the material caused by local heating during the vaporization process. However, the duration of the cut is drastically increased due to the use of low power [33,34]. This recipe is highly suitable to cut small features. Secondly, the base in green is fabricated with a rough cut to decrease fabrication time. This recipe causes much local material degradation and would therefore not be suitable for small features. Thirdly, text (purple) is engraved on the base. Often, this text contains the first four parameters in Table I, the date and designer. Additionally, design specifications and reference circles are engraved. To engrave readable text, the precession mode should be shut off.

Cut	Scanning velocity (mm/s)	Repetition rate ($\times 10^3$)	Pulse rate (kHz)	Power (%)	Power (W)	Duration (min)
Rough	500	1.45	75	60	9	3
Smooth	600	30	37.5	8	1.2	24
Text	100	5	75	3	0.45	-

TABLE I: Parameters to cut a 20 µm trench in a monocrystalline silicon wafer with a width of 380 µm: scanning velocity, repetition rate, pulse rate, power and duration. Parameters are given for a rough and fast cut of the base and a precise and smooth cut of the resonator, shown on resonators using engraving. A precession mode at $65°$ with an angular velocity of 25000 rpm is used.

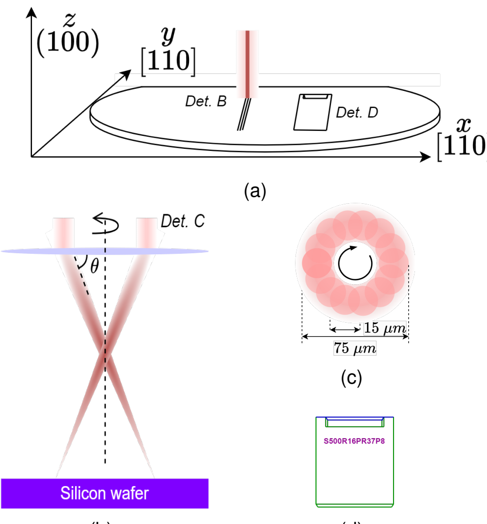

Fig. 4: Schematics of the operation of the Lasea femtosecond laser cutter. (a) Fabrication set-up with wafer orientation [32] including the femtosecond laser along one of three lines with a pitch of 10 µm between lines. (b) The use of precession with an angle of attack of $65°$ resulting in a ring shape with a diameter of 60 µm and spot diameter of 15 µm. Thus, the total thickness of a line (trench) is 80 µm. (c) Illustration of the ring-shaped laser spot due to precession of the laser. (d) The different line colours of the micromechanical resonator correspond with the parameters presented in Table I with green for a rough cut, blue for a smooth cut and purple for engraving.

This recipe is used to fabricate multiple devices at small (µm) scale. Four of these resonators are shown in Figure 5. Figure 5a and Figure 5b show two doubly clamped beams spanning 6 mm in length with a thickness of 62 µm for a straight beam (Figure 5a), and a minimum and maximum thickness of 40 µm and 150 µm for a notched beam (Figure 5b). Figure 5c presents the T-shaped resonator spanning 5 mm $\times$ 3 mm with a horizontal and vertical thickness of 51 µm and 15 µm. Finally, Figure 5d shows a coupled large mass resonator spanning 3 mm, where the two squares have side lengths 5.6 mm and 8.6 mm. The connecting beams are 1.6 mm in length and 67 µm in width. The resonators in Figure 5a-Figure 5c are fabricated using a uniform depth of 380 µm, while for the resonator in Figure 5d, the depth is 500 µm.

This fabrication method can achieve a high precision resonator in less than an hour without the use of a cleanroom, thus providing a suitable method for prototyping.

(a)

(b)

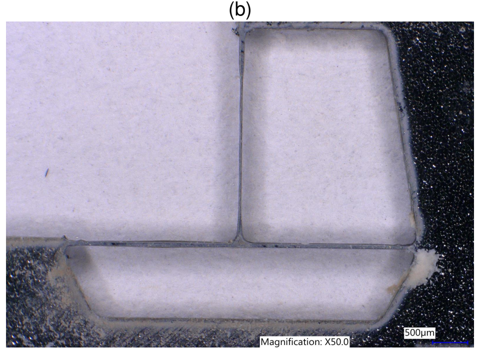

(c)

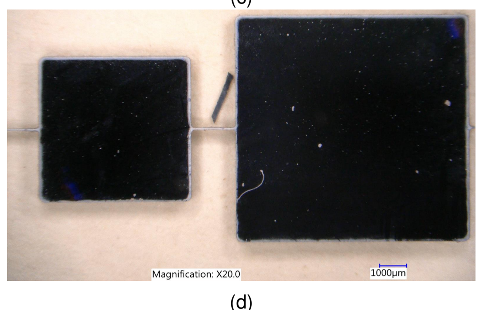

(d)

Fig. 5: Microscopic image of several micromechanical resonators fabricated using femtosecond laser vaporization of monocrystalline silicon [32]. (a, b) Doubly clamped beams [31] spanning 6 mm in length. (c) T-shaped resonator [24] spanning 5 mm $\times 3$ mm. (d) Coupled large mass resonators [15] spanning 30 mm in length.

IV. MEASUREMENT BY LASER DOPPLER VIBROMETER

To show good agreement between FEM and ROM simulations and experiments, the doubly clamped beam is measured in subsection IV-A. Thereafter, the T-shaped resonator is characterised in subsection IV-B. In subsection IV-C autoparametric coupling in the T-shaped resonator will be presented.

Actuation for both characterisation and operation is done by base excitation and provided by a piezo shaker with a maximum applied voltage of 100 V which is resonating the micromechanical resonator vertically (in-plane) as shown in Figure 6. The velocity of one or multiple points on each beam (in-plane) are detected using a Polytec MSA-400 Laser Doppler Vibrometer. Multiple points are used to characterise the frequency spectrum and eigenmodes to verify the FEM simulations. Single point measurements are used to determine modal parameters by sweeping ω_d for different magnitudes of V. Both measurements require different runs for each beam due to the single point laser. Modal frequencies and Q-factors listed in Table II are measured at drive signal of $100V$ in vacuum (10^{-4} mbar).

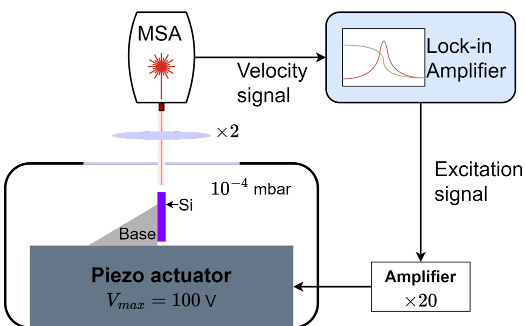

Fig. 6: Schematic of the measurement set-up comprising of a Polytec MSA-400 LDV and Lock-in Amplifier for reading-out the motion and a piezo actuator in a vacuum chamber for generating the excitation force with a maximum voltage of 100 V [28,29].

A. Characterisation of a doubly clamped beam resonator

Table II presents the natural frequency for a straight (Figure 5a) and notched (Figure 5b) clamped-clamped microbeam at a driving voltage of 100 V in vacuum, with complementary frequency sweeps in Appendix C. While Li. *et al.* [31] have excellent agreement between the numerical and measured frequency response in a microbeam fabricated by DRIE, the measured frequency in this experiment increases by approximately 1.8 due to local heating caused by laser vaporization. The local heating generates residual stress, thus increasing the resonance frequency.

Similar to Li. *et al.* where the natural frequency decreases by a factor 1.6 due to a change in beam shape, the decrease in frequency in this experiments is by a factor of 1.9. The relative high decrease could be caused by the degradation of the thinner beams, since the depth of degradation is closer to the beam thickness. However the shift in frequency appears to yield the same factor for each vibrational mode.

C-C beam	Beam thickness (µm)	Numerical frequency (kHz)	Measured frequency (kHz)	Quality factor Q ($\times 10^3$)
Straight	62	13.3	24.8	0.43
Notched	40	7.52	13.0	0.25
T-shape	Beam thickness (µm)	Numerical frequency (kHz)	Measured frequency (kHz)	Quality factor Q ($\times 10^3$)
Mode 1	80	49.7	55.5	0.28
Mode 3	36	99.5	111	0.06

TABLE II: Parameters of the microbeam and T-shaped resonators: beam thickness, numerical and measured resonance frequency, and measured quality factor. Actuation is achieved by a piezo shaker with a signal of $V = 100$ V in vacuum.

B. Characterisation of a T-shaped resonator

A T-shaped resonator is experimentally measured by using multiple points on a horizontal beam to determine the resonance frequencies and mode shapes. The resonator is measured in vacuum with a driving force of 100 V and positioned in the vacuum chamber as shown in Figure 7b. The resulting frequency response for the horizontal beam of a T-shaped resonator is shown in Figure 7, including the first three vibrational modes of the T-shaped resonator at 56 kHz, 79 kHz and 111 kHz. The corresponding resonance frequencies and mechanical quality factors for the first and third mode with associated beam thickness are given in Table II. Similarly, a measurement of the vertical beam would show a resonance frequency at 56 kHz and 79 kHz, but not a distinct peak at 111 kHz. Vertically, the modes are measured over the full vertical beam length, while the horizontal vibrational modes are measured along half a horizontal beam. The measured modeshapes are shown in Appendix C.

Similarly to subsection IV-A, the resonance frequency in both modes increases. However, the increase in natural frequency in both modes due to residual stress is by a factor of 1.12.

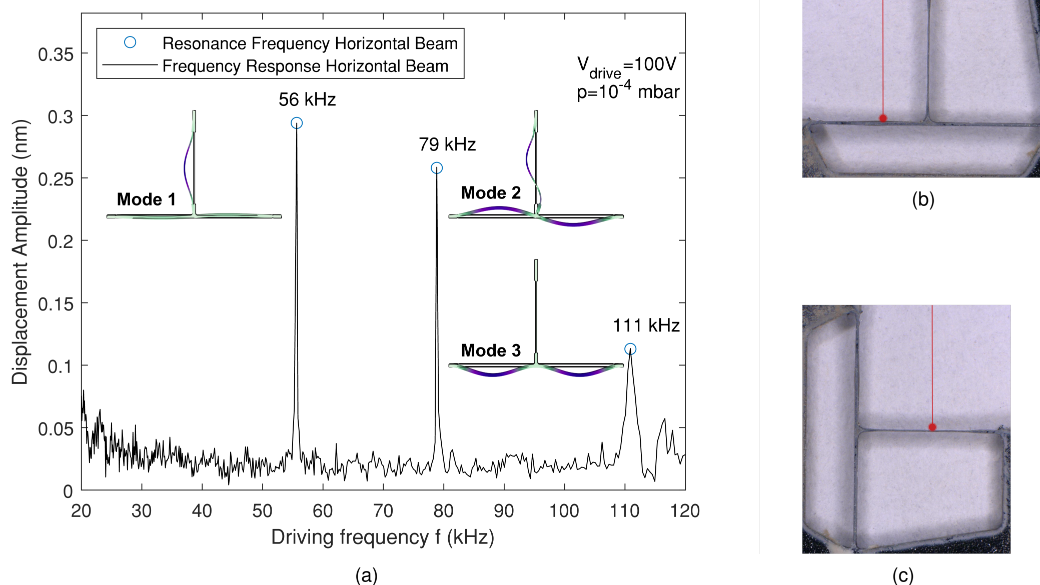

Fig. 7: Experimental characterisation of the T-shaped resonators. (a) Frequency responses measured by the LDV set-up in Figure 6 of the horizontal beam of the T-shaped resonator, respectively. Included are the first three vibrational modes of the T-shaped resonator determined by a FEM in COMSOL and confirmed in Polytec. (b, c) Microscopic images of the T-shaped resonator, positioned for measurements in the set-up. The horizontal (b) and vertical (c) beams of the T-shaped resonator span 5000 µm and 3000 µm in length and 80 µm and 36 µm in thickness, respectively, with a uniform depth of 380 µm.

C. Autoparametric coupling in a T-shaped resonator

In order to measure autoparametric resonance, a similar measurement procedure to subsection IV-B is performed. In vacuum and with a driving force of 100 V, single point measurements of the beams of the T-shaped resonator in Figure 7b and Figure 7c are taken at the marked location. At this location, the deflection of the respective mode is at a maximum as determined by numerical and experimental mode shapes. The resonator is driven at the resonance frequency of the third mode (111 kHz), which is twice the resonance frequency of the first mode (55.5 kHz).

A measurable response of the first mode in the vertical beam is observed when the amplitude of the drive signal (≥ 60 V) is sufficiently large as shown in Figure 8. At the driving frequency represented by the dotted line, the motion of the horizontal mode induces a parametric resonant response in the vertical beam. For low voltages (≤ 40 V) however, motion in the vertical beam does not occur in the T-shaped resonator. Thus, at a sufficient driving force and a frequency ratio of $f_2 = 2f_1$, autoparametric coupling is shown in the T-shaped resonator. Furthermore, the quality factor of the resonator is sufficiently high to allow for autoparametric coupling [12].

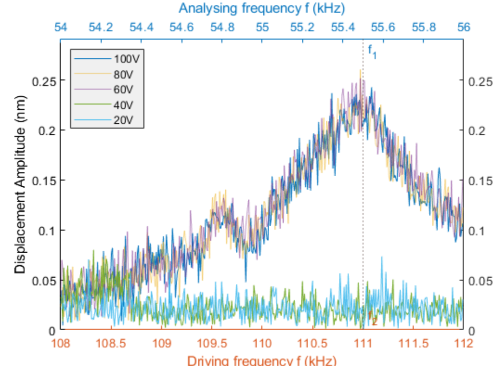

Fig. 8: Measured frequency response by the LDV in vacuum (10^{-4} mbar) of the vertical beam of a T-shaped resonator with a vertical and horizontal beam thickness of 36 µm and 80 µm, respectively. A varying drive signal of 20 V to 100 V is applied, while the vertical beam is driven at twice its resonance frequency and analysed at its resonance frequency. At a sufficient drive voltage (≥ 60 V), the vertical beam shows a distinct increase in displacement amplitude.

Additionally, a comparison can be drawn between the numerical and experimental results. The horizontal beam is driven and analysed at resonance ($f_2 = 111$ kHz) as shown in Figure 9a. The vertical beam is driven at twice its resonance ($2f_1 = 111$ kHz), which is equal to the resonance frequency of the horizontal beam, and analysed at its own resonance frequency ($f_1 = 55.5$ kHz) as shown in Figure 9b.

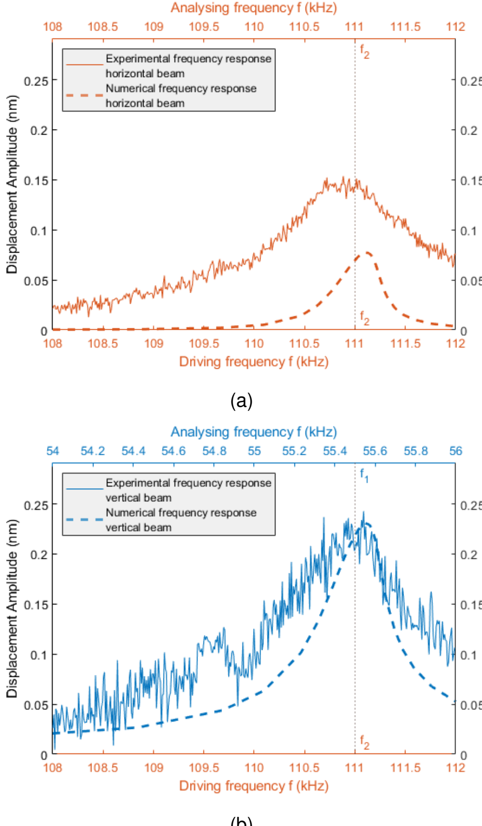

Fig. 9: Measured frequency responses by the LDV in vacuum (10^{-4} mbar) for a T-shaped resonator with a vertical and horizontal beam thickness of 36 µm and 80 µm, respectively. (a) Measured and simulated frequency response of the horizontal beam at a drive signal of 100 V, while driving and analysing at its resonance frequency (111 kHz). (b) Measured and simulated frequency response of the vertical beam at a drive signal of 100 V, while driving at twice its resonance frequency and analysing at its resonance frequency (55.5 kHz). Autoparametric coupling between the first eigenmodes of the horizontal beam and the vertical beam is thus shown to occur at a sufficient drive voltage when $f_2 = 2f_1$.

The numerical results in both figures determined by ROM are in good agreement when fitted to the frequency and force. Both results show a higher displacement amplitude of the vertical beam with respect to the displacement amplitude of the horizontal beam. According to the experimental results however, a higher horizontal displacement amplitude - and thus driving force - is necessary to achieve a similar vertical displacement amplitude.

V. CONCLUSION

During this thesis, a protocol for fabricating micromechanical resonators has been formulated. The protocol includes computational analysis by using a finite element model and a reduced order model to simulate the eigenmodes and frequency response of the resonators. Furthermore, the resonators are fabricated by femtosecond laser vaporization and measured using a laser Doppler vibrometer and lock-in amplifier.

The protocol has been validated by reproducing previous work on a microbeam resonator fabricated by dry reactive ion etching and comparing the results. The results are in good agreement concerning the expected frequency decrease due a change in the beam shape. However, the laser vaporization causes the frequency to increase sharply due to locally heating of the material which adds prestress. The frequency increase is similar for higher modes, therefore only the first mode has to be determined. A piezo actuator with a higher voltage should also be able to show a (clear) nonlinear frequency response.

The protocol has been used to fabricate a T-shaped resonator which achieves autoparametric coupling in simulations. Autoparametric coupling has been measured for a sufficiently large driving force at twice the frequency of the first mode, equal to the frequency of the second mode.

In conclusion, a protocol for fabricating and measuring micromechanical resonators has been developed to accelerate prototyping, accessing three dimensional resonators and circumventing clean rooms. Secondly, autoparametric resonance in a T-shaped resonator has been experimentally proven when the drive signal is sufficiently large and the resonance frequencies of two modes is close to $1:2$. Further investigation of the effect of femtosecond laser vaporization to the change of material properties could improve the agreement between simulation and experimental results by a) providing matching material data to the finite element model, and b) increasing the material quality by decreasing the local material change caused by femtosecond laser vaporization.

References

[1] R. P. Feynman, “There’s plenty of room at the bottom,” *Engineering and Science*, vol. 23, no. 5, pp. 22–36, 1960.

[2] M. L. Roukes, “Nanoelectromechanical systems face the future,” *PhysicsWorld*, vol. 14, 2001.

[3] ——, “Plenty of room, indeed,” *Scientific American*, vol. 285, pp. 48–51, 54, 10 2001.

[4] M. I. Younis, *MEMS Linear and Nonlinear Statics and Dynamics*. Springer Science+Business Media, LLC, 2011, vol. Microsystems 20. [Online]. Available: http://www.springer.com/series/6289

[5] R. Lifshitz and M. C. Cross, *Nonlinear Dynamics of Nanomechanical and Micromechanical Resonators*. Wiley-VCH Verlag GmbH & Co. KGaA, 12 2009.

[6] R. M. Lin and W. J. Wang, “Structural dynamics of microsystems - current state of research and future directions,” pp. 1015–1043, 7 2006.

[7] K. L. Ekinci and M. L. Roukes, “Nanoelectromechanical systems,” *Review of Scientific Instruments*, vol. 76, 2005.

[8] N. Kacem, S. Hentz, D. Pinto, B. Reig, and V. Nguyen, “Nonlinear dynamics of nanomechanical beam resonators: Improving the performance of nems-based sensors,” *Nanotechnology*, vol. 20, 2009.

[9] A. Ghosh, *Scaling Laws*. Springer New York, 2011.

[10] D. M. Farhadi, *Compliant transmission mechanisms*, 2018. [Online]. Available: https://doi.org/10.4233/uuid:865dce30-2133-4e1a-add9-f0cb4ba4b3c4

[11] L. L. Howell, *Compliant mechanisms. 21st Century Kinematics: The 2012 NSF Workshop*. Springer London, 2013.

[12] P. G. Steeneken, R. J. Dolleman, D. Davidovikj, F. Alijani, and H. S. V. D. Zant, “Dynamics of 2d material membranes,” *2D Materials*, vol. 8, 10 2021.

[13] S. I. Chang, A. K. Bajaj, and C. M. Krousgrill, “Non-linear vibrations and chaos in harmonically excited rectangular plates with one-to-one internal resonance,” 1993.

[14] S. H. Nitzan, V. Zega, M. Li, C. H. Ahn, A. Corigliano, T. W. Kenny, and D. A. Horsley, “Self-induced parametric amplification arising from nonlinear elastic coupling in a micromechanical resonating disk gyroscope,” *Scientific Reports*, vol. 5, 2015.

[15] Y. Yan, X. Dong, L. Huang, K. Moskovtsev, and H. B. Chan, “Energy transfer into period-tripled states in coupled electromechanical modes at internal resonance,” *Physical Review X*, vol. 12, 7 2022.

[16] A. Sarrafan, S. Azimi, F. Golnaraghi, and B. Bahreyni, “A nonlinear rate microsensor utilising internal resonance,” *Scientific Reports*, vol. 9, 12 2019.

[17] F. Golnaraghi, B. Behreyni, A. Marzouk, A. Sarrafan, S. A. M. Lajimi, O. Pooyanfar, and N. Noori, U.S. Patent 15/799,922, 2018.

[18] C. Lan, W. Qin, and W. Deng, “Energy harvesting by dynamic unstability and internal resonance for piezoelectric beam,” *Applied Physics Letters*, vol. 107, 8 2015.

[19] A. H. Ramini, A. Z. Hajjaj, and M. I. Younis, “Tunable resonators for nonlinear modal interactions,” *Scientific Reports*, vol. 6, 10 2016.

[20] D. Antonio, D. H. Zanette, and D. López, “Frequency stabilization in nonlinear micromechanical oscillators,” *Nature Communications*, vol. 3, 2012.

[21] A. Keşkekler, H. Arjmandi-Tash, P. G. Steeneken, and F. Alijani, “Symmetry-breaking-induced frequency combs in graphene resonators,” *Nano Letters*, vol. 22, pp. 6048–6054, 8 2022.

[22] N. Noori, A. Sarrafan, F. Golnaraghi, and B. Bahreyni, “Utilization of 2:1 internal resonance in microsystems,” *Micromachines*, vol. 9, 2018.

[23] K. R. Qalandar, B. S. Strachan, B. Gibson, M. Sharma, A. Ma, S. W. Shaw, and K. L. Turner, “Frequency division using a micromechanical resonance cascade,” *Applied Physics Letters*, vol. 105, 12 2014.

[24] S. Dou, B. S. Strachan, S. W. Shaw, and J. S. Jensen, “Structural optimization for nonlinear dynamic response,” *Philosophical Transactions of the Royal Society A: Mathematical, Physical and Engineering Sciences*, vol. 373, 9 2015.

[25] M. Wang, D. Ge, L. Zhang, and J. L. Herder, “Micro-scale realization of compliant mechanisms: Manufacturing processes and constituent materials—a review,” *Chinese Journal of Mechanical Engineering (English Edition)*, vol. 34, 12 2021.

[26] Z. Lei, Y. Chen, G. Xu, J. Liu, M. Yuan, L. Zeng, X. Ji, and D. Wu, “Micromachining of high quality pmn-31

[27] B. S. Strachan, S. W. Shaw, and O. Kogan, “Subharmonic resonance cascades in a class of coupled resonators,” *Journal of Computational and Nonlinear Dynamics*, vol. 8, 2013.

[28] Z. Li, M. Xu, R. A. Norte, A. M. Aragón, F. V. Keulen, F. Alijani, and P. G. Steeneken, “Tuning the q -factor of nanomechanical string resonators by torsion support design,” *Applied Physics Letters*, vol. 122, 1 2023.

[29] Z. Li, M. Xu, R. A. Norte, A. M. Aragón, P. G. Steeneken, and F. Alijani, “Strain engineering of nonlinear nanoresonators from hardening to softening,” *Communications Physics*, vol. 7, 12 2024.

[30] V. Bos and P. G. Steeneken, “Nonlinear dynamics of graphene membranes quality factor limits of membranes caused by mode in-teraction,” 2020.

[31] L. L. Li, P. M. Polunin, S. Dou, O. Shoshani, B. S. Strachan, J. S. Jensen, S. W. Shaw, and K. L. Turner, “Tailoring the nonlinear response of mems resonators using shape optimization,” *Applied Physics Letters*, vol. 110, 2 2017.

[32] M. A. Hopcroft, W. D. Nix, and T. W. Kenny, “What is the young’s modulus of silicon?” *Journal of Microelectromechanical Systems*, vol. 19, pp. 229–238, 4 2010.

[33] J. Lopez, M. Faucon, R. Devillard, Y. Zaouter, C. Honninger, E. Mottay, and R. Kling, “Parameters of influence in surface ablation and texturing of metals using high-power ultrafast laser,” *Journal of Laser Micro Nanoengineering*, vol. 10, pp. 1–10, 2015.

[34] L. Cangueiro, J. A. Ramos-De-campos, and D. Bruneel, “Prediction of thermal damage upon ultrafast laser ablation of metals,” *Molecules*, vol. 26, 11 2021.

5
Outlook

The objectives of this work have been to formulate a protocol to fabricate micromechanical resonators by femtosecond laser vaporization and determine autoparametric resonance in certain resonators. This section reports on the conclusion of these objectives and recommendations for future work.

5.1. Conclusion

To conclude this master's thesis, the two objectives will be examined. Firstly, the protocol has been validated by reproducing previous work on a microbeam resonator fabricated by dry reactive ion etching and comparing the results. Secondly, the protocol has been used to fabricate a T-shaped resonator which achieves autoparametric coupling in simulations.

Validation of the fabrication and measurement protocol Several micromechanical resonators have been fabricated with a minimum feature thickness of several tens of micrometers. The minimum feature size is still larger then conventional methods such as DRIE have achieved. However, femtosecond laser vaporization can be used for fast prototyping of micromechanical resonators without the use of a clean room and has the potential to fabricate three dimensional structures.

Subsequently, three resonators (two doubly clamped beams and a T-shaped resonator) have been measured with a laser Doppler vibrometer and lock-in amplifier to validate the formulated protocol by comparing the results to a computational analysis. The computational analysis includes a finite element model and a reduced order model to simulate the eigenmodes and frequency response of the resonators.

The results of the experiments are in good agreement to the simulations concerning the expected frequency decrease due a change in the beam shape. However, the laser vaporization causes the frequency to increase sharply due to locally heating of the material which adds prestress. This effect is especially noticeable in doubly clamped beams and less profound in the T-shaped resonator. In the former case, the resulting increase

in frequency can be twice the numerical calculated frequency, while the frequency of the latter case is approximately 10 %.

Autoparametric coupling The formulated and validated protocol has been used to fabricate the T-shaped resonator to achieve autoparametric coupling, which has been shown to occur in simulations. Autoparametric coupling has also been experimentally measured for a sufficiently large driving force at twice the frequency of the first mode, equal to the frequency of the second mode.

5.2. RECOMMENDATIONS

Recommendations could mainly be given for two parts of the protocol, femtosecond laser vaporization and laser Doppler vibrometry. These two techniques have been extensively used in this master's thesis.

Femtosecond laser vaporization As shown in multiple devices, the vaporization process has a profound effect on the material of the resonator. This has been concluded by the affected frequency responses of these resonators. Further investigation of the effect of femtosecond laser vaporization to the change of material properties could improve the agreement between simulation and experimental results by a) providing matching material data to the finite element model, and b) increasing the material quality by decreasing the local material change.

Due to local heating, the material could hypothetically liquify and harden, resulting in prestress in the resonator. This thesis has investigated this hypothesis, but it could be interesting to study in particular. Noteworthy, the frequency increase is remarkably similar for higher modes, therefore only the first mode has to be determined.

Additionally, the effect of laser vaporization on different materials could be worthwhile to study since many micromechanical devices are often fabricated from silicon wafers with added impurities.

Furthermore, the fabrication of several different micromechanical resonators which are conventionally fabricated by DRIE, could show similar results

Lastly, a cleaning procedure such as ultra-sonic cleaning removes debris, while hydro florid etching also removes silicon-dioxide (the changed material after laser vaporization). However, cleaning procedures increase clean room use and slow the prototyping process.

Laser Doppler Vibrometry One recommendation concerning LDV is the increase in voltage output, which should be increased in order to show clear hardening or softening in resonators and decrease the signal to noise ratio.

Furthermore, damping due to clamping of the material could still be problematic. A recommendation concerning damping would be to change the clamping method. Since the Quality factor is dependent on the frequency, the damping could also be decreased by an increase in frequency by either a different material with prestress or a higher Young's modulus.

Lastly, the phase data should be recorded in order to improve the observation of mode coupling since a phase shift will occur due to coupling.

Additional recommendations Lastly, while a comparison of a doubly clamped microbeam fabricated by different methods has been done, a similar comparison of the T-shaped resonator could results in quantitative of the fabrication duration and difference in measurement results.

Concluding, femtosecond laser vaporization proves to be an interesting and promising fabrication technique to fabricate intricate, three dimensional micromechanical resonators exhibiting highly nonlinear phenomena such as autoparametric coupling, reducing clean room use.

6

SELF REFLECTION

According to the *Vision on Education* by TU Delft [38], it is paramount for an engineer to master certain core competences. These are:

1. Critical thinking and reflection,
2. Designing,
3. Developing an academic approach,
4. Communication and collaboration in interdisciplinary and intercultural teams,
5. Taking into account the temporal and social context of technological solutions.

A master thesis and its course is an excellent moment to evaluate a students mastery of these components. To start this self reflection on this work and performance, the author shall adhere to the first and third principles throughout this self reflection.

Furthermore, the TU Delft values a certain knowledge triangle [39] with regards to strategy towards its students and research. This concerns education, research and valorisation. Education describes both the traditional education such as courses, but also the learning curve during the thesis. Research is characterised primarily by the value added to the research community. Valorisation "*is the process of creating value from scientific knowledge, by making it suitable and/ or available for economical and/ or social exploitation and to translate it into innovative products, services, processes and new business to benefit society & public health*" [40]. Within this context, this project has not been used to create economical or social value. Thus, this self reflection shall be focused on education and research.

EDUCATION

During and before this master thesis, the author completed courses on several subject in high-tech engineering. Several of these courses have been used in this thesis in some

extend. Especially courses such as *Engineering Dynamics*, *Nonlinear Mechanics*, *Nonlinear Dynamics* and *Compliant Mechanics* were reviewed at the start of this master's thesis. Furthermore, the author has been a student assistant for four years for multiple BSc and MSc courses, which have both amplified his own understanding of several concepts in mechanical engineering and gained proficiency in teaching and other soft skills that have been proven to be useful during this project.

On the other hand, experience with hardware was limited at the start of this project. After a year, the author has gained extensive experience with the Lasea femtosecond laser cutter, laser Doppler vibrometery, Keyence digital microscope and instruments such as a Lock-in amplifier. Importantly, the use of a cleanroom has been included in this thesis.

Additionally, this thesis had led to experience with concepts and applications of reduced order modelling from finite element simulations to simulate frequency response curves to identify nonlinearity and mode coupling in MEMS.

Finally, the author has developed a strong academic approach due this thesis. Reflecting back on the past year, understanding and experience in the field of microdynamics has been strongly improved. It seems only fitting to close of with a quote by Søren Kierkegaard:"*Life can only be understood backwards; but it must be lived forwards*".

Timeline & Protocol Equal to the previously established protocol (see Figure 6.1), a timeline can be created of this thesis. This timeline, shown in Table 6.1, has been largely established at the start of this master's thesis. Although, the project has been inevitably delayed due to faulty equipment or mistakes that have led to an incredible learning curve and expectation management.

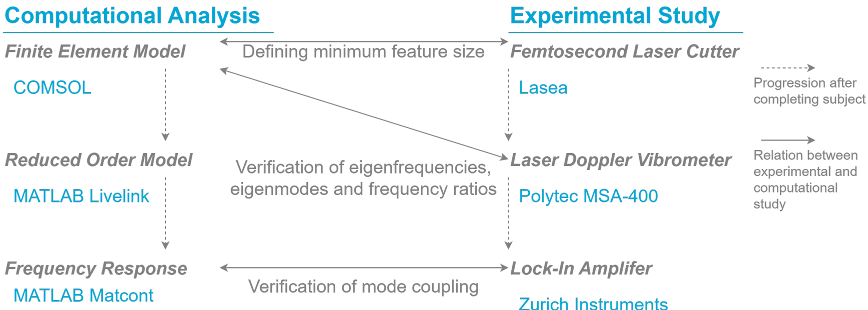

Figure 6.1: Protocol to fabricate and measure micromechanical resonators by using a combination of software and hardware.

Month	Phase	Progress
Feb ’23	Literature Review	Start of Project
Mar ’23	Literature Review	Equipment training
Apr ’23	Fabrication & Literature Review	First fabrication of simple resonators (beams)
May ’23	Fabrication	Successful fabrication of simple resonators (beams)
Jun ’23	Simulation*	Simulation of nonlinear curves in various resonators via ROM
Jul ’23	Simulation*	Simulation of mode coupling in various resonators via ROM
Aug ’23	Simulation*	Simulation and determination of suitable resonator
Sep ’23	Fabrication	Fabrication of resonator
Okt ’23	Fabrication & experimentation	Fabrication and measurements of resonator
Nov ’23	Fabrication & experimentation	Fabrication and measurements of resonator
Dec ’23	Fabrication & experimentation	Fabrication and measurements of resonator
Jan ’23	Experimentation	Measurements of resonator and fitting to simulations
Feb ’24	Thesis	Finishing thesis

Table 6.1: Timeline of this master’s thesis

*During the three month period June - Augustus, the femtosecond laser was unfortunately been broken.

Research

The main contribution of this thesis is the formulation of a protocol to fabricate using femtosecond laser vaporization, and measure using laser Doppler vibrometry, microscale resonators. This protocol has been validate by showing several interesting phenomena in these resonators.

This research has been done by following a protocol similar to Keşkekler *et al.* [22] with regards to the combination of computational analysis and measurements and Li *et al.* [27] concerning the laser Doppler vibrometry. Furthermore, validation of the protocol in this thesis has been based upon previous work [41] and used to determine mode coupling in an already develop model by Dou *et al.* [24].

Research Community The protocol that has been developed, is suitable for projects concerning the fabrication of microsystems by femtosecond laser vaporization. The insights offered by this paper and expertise provided by the author has already been used by several (PhD) students. Of course, during the development of new microsystems, the

protocol has to be adjusted specifically for the demands of certain materials, geometries and applications. However, this protocol proves to provide a starting point for new projects involving femtosecond laser vaporization.

Bibliography

1. Feynman, R. P. There's Plenty of Room at the Bottom. *Engineering and Science* **23,** 22–36 (1960).
2. Roukes, M. L. Nanoelectromechanical systems face the future. *PhysicsWorld* **14** (2 2001).
3. Roukes, M. L. Plenty of Room, Indeed. *Scientific American* **285,** 48–51, 54 (Oct. 2001).
4. Younis, M. I. *MEMS Linear and Nonlinear Statics and Dynamics* ISBN: 978-1-4419-6019-1. http://www.springer.com/series/6289 (Springer Science+Business Media, LLC, 2011).
5. Lifshitz, R. & Cross, M. C. *Nonlinear Dynamics of Nanomechanical and Micromechanical Resonators* 2. ISBN: 9783527407293 (Wiley-VCH Verlag GmbH & Co. KGaA, Dec. 2009).
6. Lin, R. M. & Wang, W. J. *Structural dynamics of microsystems - Current state of research and future directions* July 2006.
7. Ekinci, K. L. & Roukes, M. L. Nanoelectromechanical systems. *Review of Scientific Instruments* **76.** ISSN: 00346748 (6 2005).
8. Kacem, N., Hentz, S., Pinto, D., Reig, B. & Nguyen, V. Nonlinear dynamics of nanomechanical beam resonators: Improving the performance of NEMS-based sensors. *Nanotechnology* **20.** ISSN: 09574484 (27 2009).
9. Ghosh, A. *Scaling Laws* 61–94 (Springer New York, 2011).
10. Farhadi, D. M. *Compliant transmission mechanisms* https://doi.org/10.4233/uuid:865dce30-2133-4e1a-add9-f0cb4ba4b3c4 (2018).
11. Howell, L. L. *Compliant mechanisms. 21st Century Kinematics: The 2012 NSF Workshop* 189–216. ISBN: 978-1-4471-4509-7 (Springer London, 2013).
12. Steeneken, P. G., Dolleman, R. J., Davidovikj, D., Alijani, F. & Zant, H. S. V. D. Dynamics of 2D material membranes. *2D Materials* **8.** ISSN: 20531583 (4 Oct. 2021).
13. Frequency division using a micromechanical resonance cascade. *Applied Physics Letters* **105.** ISSN: 00036951 (24 Dec. 2014).
14. Chang, S. I., Bajaj, A. K. & Krousgrill, C. M. *Non-Linear Vibrations and Chaos in Harmonically Excited Rectangular Plates with One-to-One Internal Resonance* 1993.
15. Nitzan, S. H. *et al.* Self-induced parametric amplification arising from nonlinear elastic coupling in a micromechanical resonating disk gyroscope. *Scientific Reports* **5.** ISSN: 20452322 (2015).
16. Yan, Y., Dong, X., Huang, L., Moskovtsev, K. & Chan, H. B. Energy Transfer into Period-Tripled States in Coupled Electromechanical Modes at Internal Resonance. *Physical Review X* **12.** ISSN: 21603308 (3 July 2022).

17. Sarrafan, A., Azimi, S., Golnaraghi, F. & Bahreyni, B. A Nonlinear Rate Microsensor utilising Internal Resonance. *Scientific Reports* **9.** ISSN: 20452322 (1 Dec. 2019).
18. Golnaraghi, F. *et al.* 15/799,922 (2018).
19. Lan, C., Qin, W. & Deng, W. Energy harvesting by dynamic unstability and internal resonance for piezoelectric beam. *Applied Physics Letters* **107.** ISSN: 00036951 (9 Aug. 2015).
20. Ramini, A. H., Hajjaj, A. Z. & Younis, M. I. Tunable resonators for nonlinear modal interactions. *Scientific Reports* **6.** ISSN: 20452322 (Oct. 2016).
21. Antonio, D., Zanette, D. H. & López, D. Frequency stabilization in nonlinear micromechanical oscillators. *Nature Communications* **3.** ISSN: 20411723 (2012).
22. Keşkekler, A., Arjmandi-Tash, H., Steeneken, P. G. & Alijani, F. Symmetry-Breaking-Induced Frequency Combs in Graphene Resonators. *Nano Letters* **22,** 6048–6054. ISSN: 15306992 (15 Aug. 2022).
23. Noori, N., Sarrafan, A., Golnaraghi, F. & Bahreyni, B. Utilization of 2:1 internal resonance in microsystems. *Micromachines* **9.** ISSN: 2072666X (9 2018).
24. Structural optimization for nonlinear dynamic response. *Philosophical Transactions of the Royal Society A: Mathematical, Physical and Engineering Sciences* **373.** ISSN: 1364503X (2051 Sept. 2015).
25. Wang, M., Ge, D., Zhang, L. & Herder, J. L. Micro-scale Realization of Compliant Mechanisms: Manufacturing Processes and Constituent Materials—A Review. *Chinese Journal of Mechanical Engineering (English Edition)* **34.** ISSN: 21928258 (1 Dec. 2021).
26. Strachan, B. S., Shaw, S. W. & Kogan, O. Subharmonic resonance cascades in a class of coupled resonators. *Journal of Computational and Nonlinear Dynamics* **8.** ISSN: 15551415 (4 2013).
27. Li, Z. *et al.* Tuning the Q-factor of nanomechanical string resonators by torsion support design. *Applied Physics Letters* **122.** ISSN: 00036951 (1 Jan. 2023).
28. Li, Z. *et al.* Strain engineering of nonlinear nanoresonators from hardening to softening. *Communications Physics* **7.** ISSN: 23993650 (1 Dec. 2024).
29. Clerc, P. A. *et al.* Advanced deep reactive ion etching: A versatile tool for microelectromechanical systems. *Journal of Micromechanics and Microengineering* **8,** 272–278. ISSN: 09601317 (4 Dec. 1998).
30. Laermer, F., Franssila, S., Sainiemi, L. & Kolari, K. in, 444–469 (Elsevier Inc., Jan. 2015). ISBN: 9780323312233.
31. Chicbkov, B. N., Momma, C., Nolte, S., Alvensleben, F. Y. & Tiinnermann, A. *Femtosecond, picosecond and nanosecond laser ablation of solids* 1996.
32. Lopez, J. *et al.* Parameters of influence in surface ablation and texturing of metals using high-power ultrafast laser. *Journal of Laser Micro Nanoengineering* **10,** 1–10. ISSN: 18800688 (1 2015).
33. Cangueiro, L., Ramos-De-campos, J. A. & Bruneel, D. Prediction of thermal damage upon ultrafast laser ablation of metals. *Molecules* **26.** ISSN: 14203049 (21 Nov. 2021).

6

34. What is the Young's modulus of silicon? *Journal of Microelectromechanical Systems* **19,** 229–238. ISSN: 10577157 (2 Apr. 2010).

35. Abe, H., Kato, H. & Baba, T. *Specific heat capacity measurement of single-crystalline silicon as new reference material* in. **50** (Nov. 2011).

36. Mills, A. & Coimbra, C. *Basic Heat and Mass Transfer 3/E* ISBN: 978-0-9963053-0-3 (Temporal Publishing, LLC, 2015).

37. Bos, V. & Steeneken, P. G. *Nonlinear dynamics of graphene membranes Quality factor limits of membranes caused by mode in-teraction* (2020).

38. Delft, T. U. *Vision on Education* https://filelist.tudelft.nl/TUDelft/Over_TU_Delft/Strategie/Towards%20a%20new%20strategy/Vision%20on%20Education_web.pdf (2024).

39. Delft, T. U. *Interactie Onderzoek-Onderwijs-Valorisatie* https://www.tudelft.nl/over-tu-delft/strategie/interactie-onderzoek-onderwijs-valorisatie (2024).

40. Asmterdam, V. U. *Valorisation* https://vu.nl/en/employee/research-support/valorisation (2024).

41. Tailoring the nonlinear response of MEMS resonators using shape optimization. *Applied Physics Letters* **110.** ISSN: 00036951 (8 Feb. 2017).

Appendix A: Additional reduced order modelling results

To achieve autoparametric coupling, both a sufficient drive force has to be provided as well as a certain frequency ratio of the two modes. By using reduced order modelling, several different cases can be studied to determine which beam ratio shows mode coupling. In these cases, the first mode is the driven mode, while the third mode is induced by the first mode. A horizontal beam thickness of 75 µm - 80 µm show strong coupling and a significant nonlinear response.

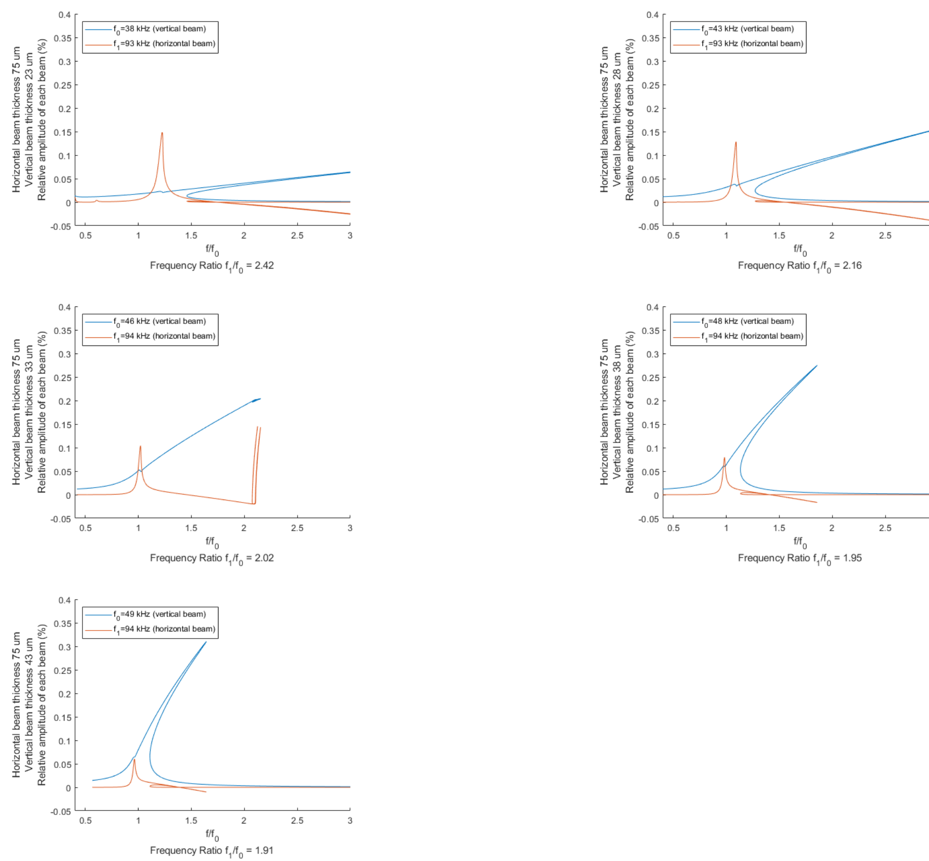

Figure A.1: Reduced Order Modelling for a horizontal beam thickness of 75 μm and a varying horizontal thickness from 23 μm and 43 μm.

A

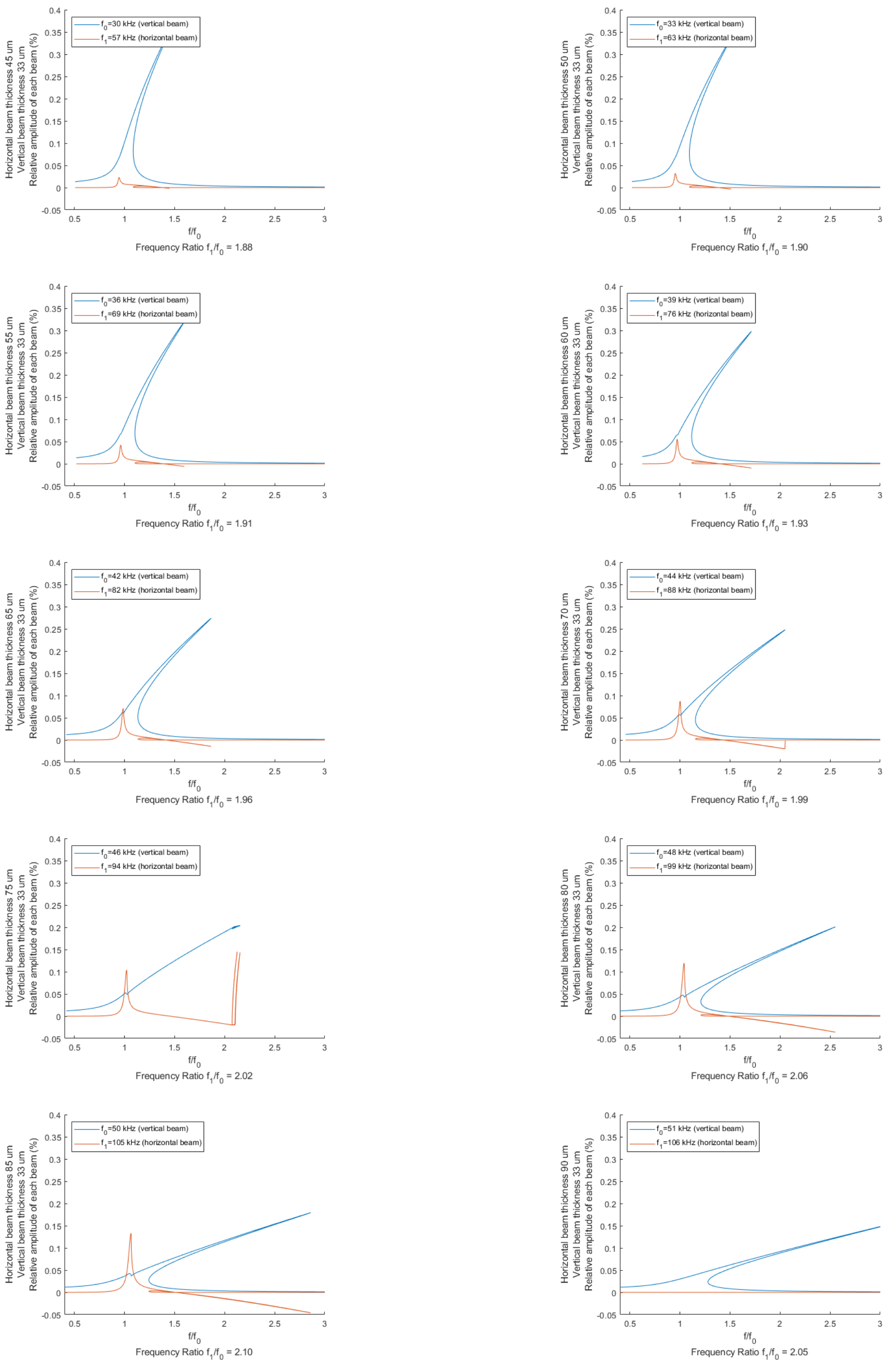

Figure A.2: Reduced Order Modelling for a vertical beam thickness of 33 μm and a varying horizontal thickness from 45 μm and 90 μm.

Appendix B: Additional fabrication results

Many structures have been cut in order to determine the fabrication parameters as shown in Table B.1. Some of the T-shaped structures are shown in this appendix including the thickness of the beams.

	Scanning velocity (mm/s)	Repetition rate ($\times 10^3$)	Pulse rate ($\times 10^3\ s$)	power (%)	Duration (min)
Rough cut	500	1.45	75	60	8
Smooth cut	600	30	37.5	8	45

Table B.1: Parameters to cut a 20 µm trench in a monocrystalline silicon wafer with a width of 380 µm: scanning velocity, repetition rate, pulse rate, power and duration. Parameters are given for a rough and fast cut of the base and a precise and smooth cut of the resonator, shown on resonators using engraving. A precession mode at 65° with an angular velocity of 25000 rpm is used.

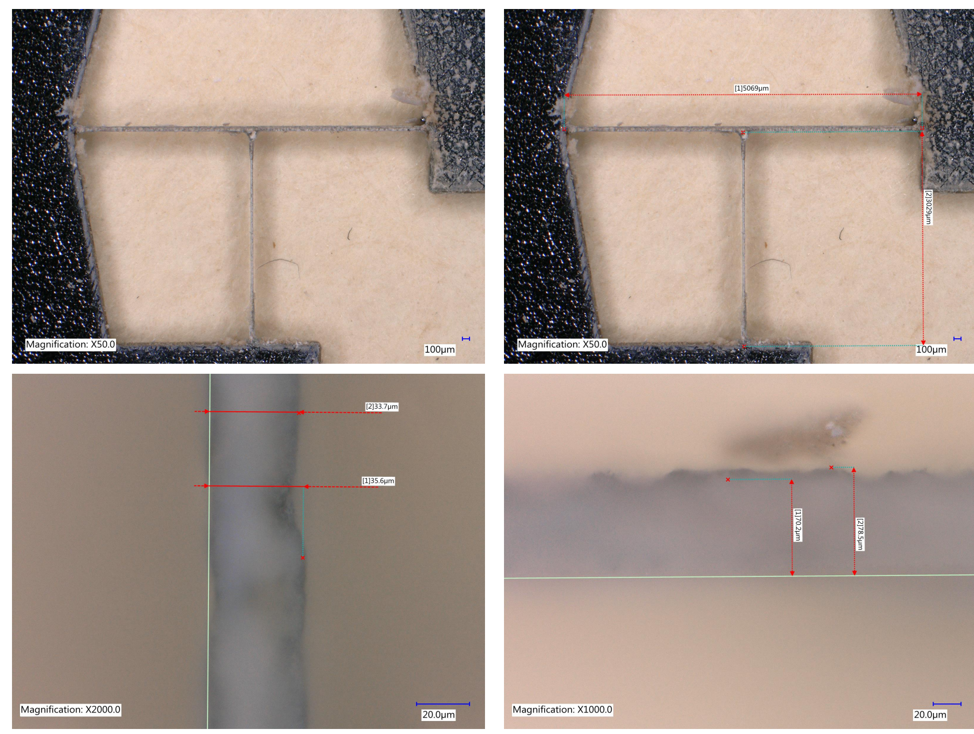

Figure B.1: A T-shaped resonator

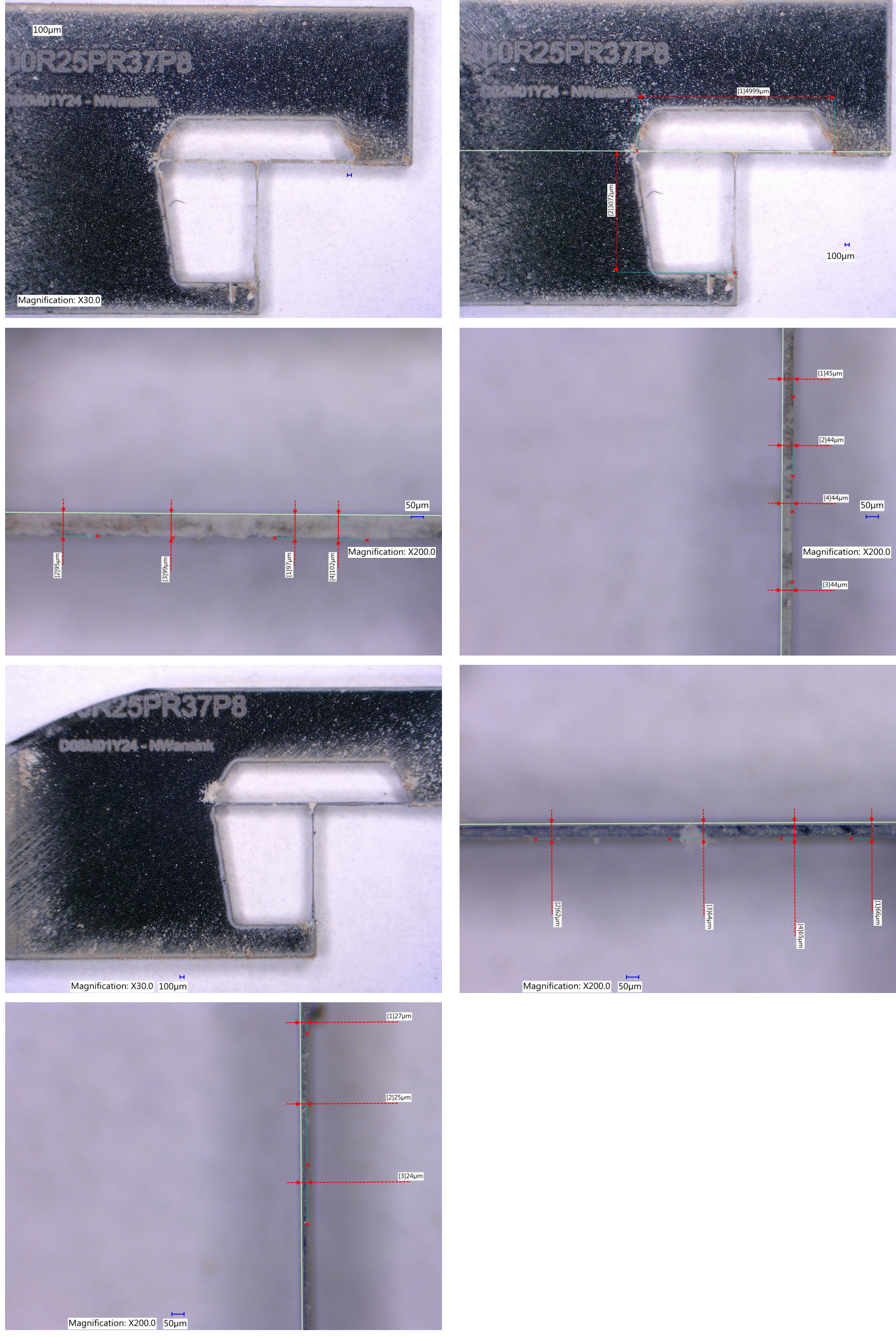

Figure B.2: Several fabricated T-shaped resonators

APPENDIX C: ADDITIONAL MEASUREMENTS RESULTS

C.1. DOUBLY CLAMPED BEAM RESONATORS

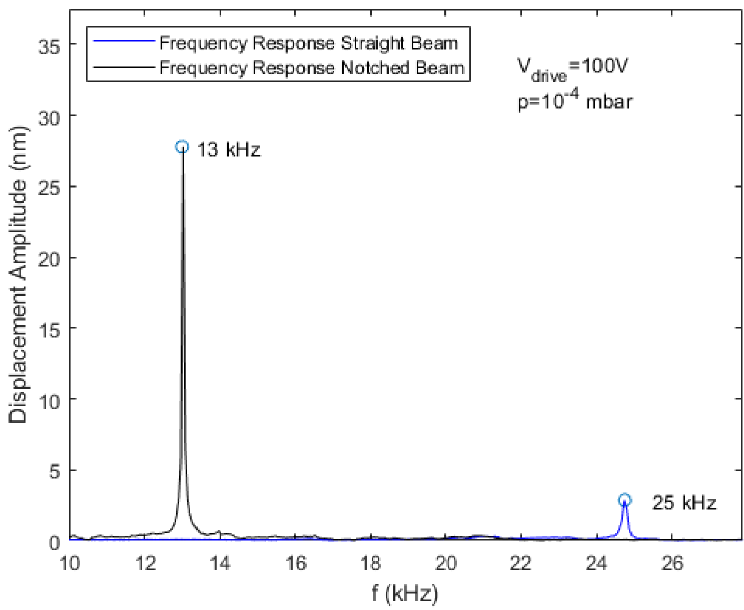

Figure C.1: Experimental characterisation of the first mode of two beam resonators with a length of 6000 µm. The thickness is 62 µm for the straight beam and 40 µm for the notched beam with 150 µm thick notches, respectively, with a uniform depth of 380 µm.

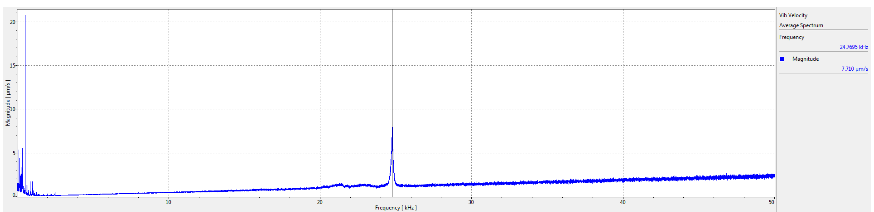

Figure C.2: Measurement in the Polytec of a straight beam showing a resonance frequency at 25 kHz

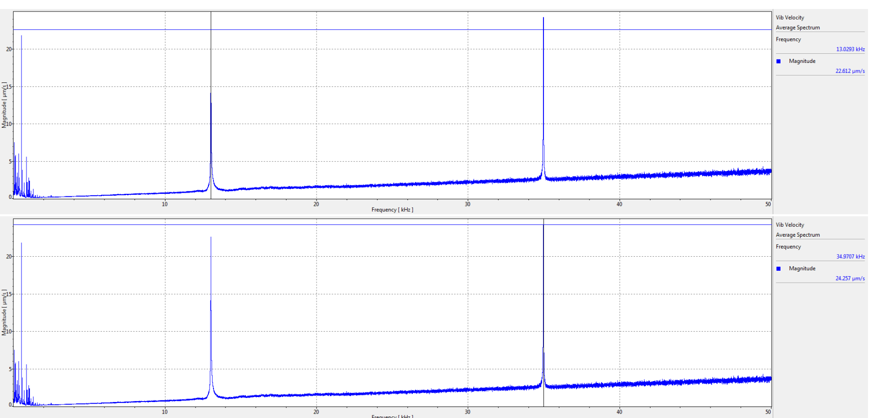

Figure C.3: Measurement in the Polytec of a notched beam showing two resonance frequency at 13 kHz and 35 khz

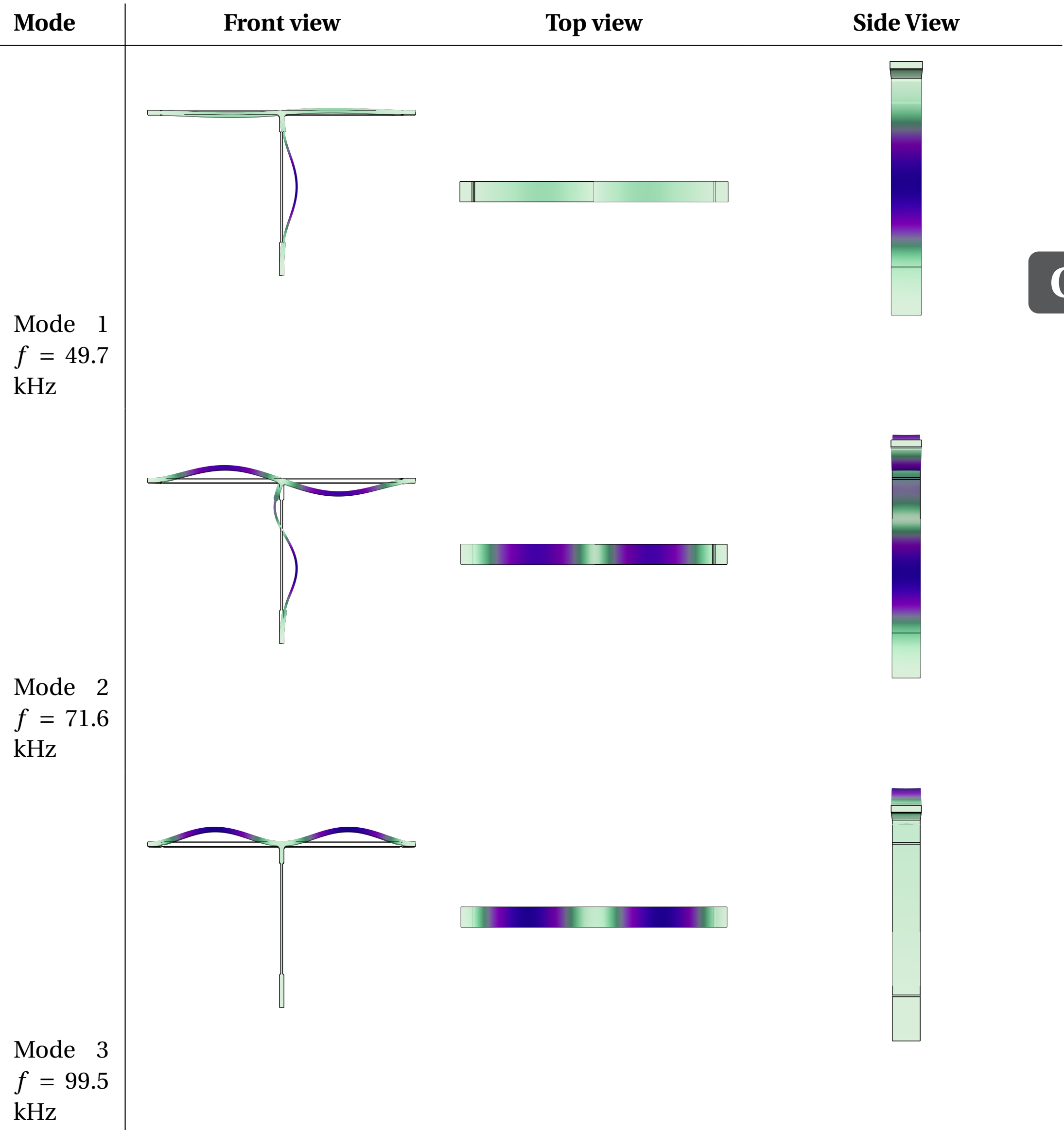

Table C.1: The first three numerical resonance frequencies and corresponding modeshapes at several views of the T-shaped resonator for a horizontal and vertical beam thickness of 80 µm and 36 µm, respectively.

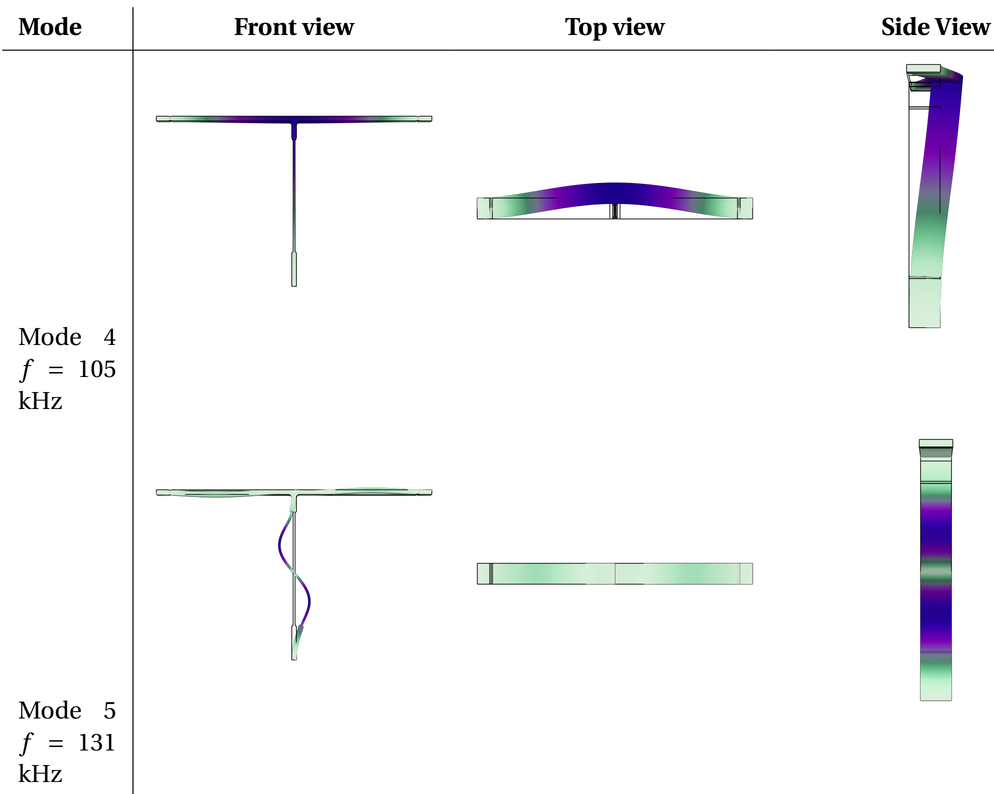

Mode	Front view	Top view	Side View
Mode 4 f = 105 kHz			
Mode 5 f = 131 kHz			

Table C.2: The fourth and fifth numerical resonance frequencies and corresponding modeshapes at several views of the T-shaped resonator for a horizontal and vertical beam thickness of 80 µm and 36 µm, respectively.

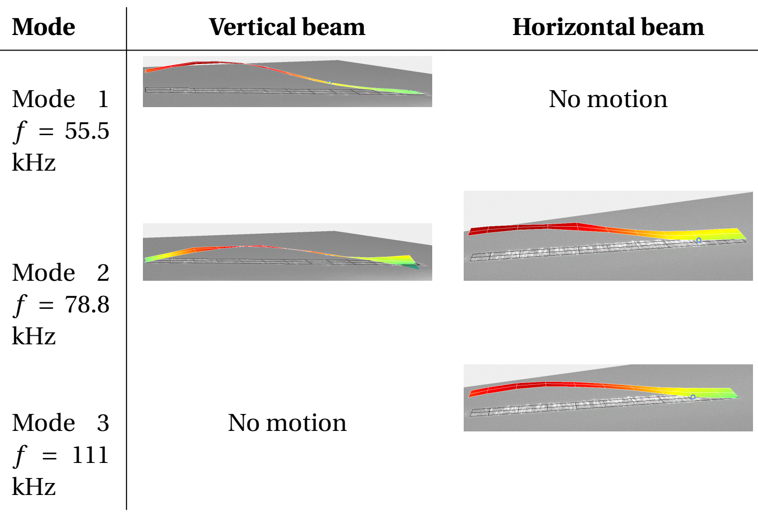

Mode	Vertical beam	Horizontal beam
Mode 1 f = 55.5 kHz		No motion
Mode 2 f = 78.8 kHz		
Mode 3 f = 111 kHz	No motion	

Table C.3: The first three experimental resonance frequencies and corresponding modeshapes at several views of the T-shaped resonator for a horizontal and vertical beam thickness of 80 µm and 36 µm, respectively. The vertical beam is clamped on the left, the horizontal beam is clamped at the right side. Only half of the horizontal beam is shown, due to the measurement method. The mode shape and their appearance are at the expected frequencies.